Journal Pre-proofs

Polymer nanotherapeutics with the controlled release of acetylsalicylic acid and its derivatives inhibiting cyclooxygenase isoforms and reducing the production of pro-inflammatory mediators

Markéta Frejková, Kateřina Běhalová, Daniela Rubanová, Juan Bautista De Sanctis, Luká š Kubala, Petr Chytil, Alice Šimonová, Tomá š Kř í žek, Eva Randárová, Kristýna Gunár, Tomá š Etrych

PII: S0378-5173(24)00976-1
DOI: https://doi.org/10.1016/j.ijpharm.2024.124742
Reference: IJP 124742

To appear in: *International Journal of Pharmaceutics*

Received Date: 2 August 2024
Revised Date: 26 August 2024
Accepted Date: 20 September 2024

Please cite this article as: M. Frejková, K. Běhalová, D. Rubanová, J. Bautista De Sanctis, L. Kubala, P. Chytil, A. Šimonová, T. Kř í žek, E. Randárová, K. Gunár, T. Etrych, Polymer nanotherapeutics with the controlled release of acetylsalicylic acid and its derivatives inhibiting cyclooxygenase isoforms and reducing the production of pro-inflammatory mediators, *International Journal of Pharmaceutics* (2024), doi: https://doi.org/10.1016/j.ijpharm.2024.124742

Polymer nanotherapeutics with the controlled release of acetylsalicylic acid and its derivatives inhibiting cyclooxygenase isoforms and reducing the production of pro-inflammatory mediators

Markéta Frejková[a], Kateřina Běhalová[a,†], Daniela Rubanová[b,c], Juan Bautista De Sanctis[d], Lukáš Kubala[b,c,e], Petr Chytil[a], Alice Šimonová[f], Tomáš Křížek[f], Eva Randárová[a], Kristýna Gunár[a], Tomáš Etrych[a*]

[a] Institute of Macromolecular Chemistry, Czech Academy of Sciences, Heyrovského náměstí 2, 162 00 Prague 6, Czech Republic.

[b] Institute of Biophysics of the Czech Academy of Sciences, Královopolská 135, 612 00, Brno, Czech Republic.

[c] Department of Experimental Biology, Faculty of Science, Masaryk University, Kamenice 5, 625 00 Brno, Czech Republic.

[d] Institute of Molecular and Translational Medicine, Faculty of Medicine and Dentistry, Palacky University, 779 00 Olomouc, Czech Republic.

[e] International Clinical Research Center – Center of Biomolecular and Cellular Engineering, St. Anne's University Hospital, Pekařská 53, 602 00, Brno, Czech Republic.

[f] Department of Analytical Chemistry, Faculty of Science of Charles University, Albertov 6, 128 00 Prague 2, Czech Republic.

†Current address: Institute of Microbiology of the Czech Academy of Sciences, v.v.i., Vídeňská 1083, 142 20 Prague, Czech Republic.

*Corresponding author: etrych@imc.cas.cz

Keywords: drug delivery, HPMA, nanotherapeutics, inflammation, acetylsalicylic acid, salicylic acid hydrazide

Abstract

The effective treatment of inflammatory diseases, particularly their chronic forms, is a key task of modern medicine. Herein, we report the synthesis and evaluation of biocompatible polymer conjugates based on *N*-2-(hydroxypropyl)methacrylamide copolymers enabling the controlled release of acetylsalicylic acid (ASA)-based anti-inflammatory drugs under specific stimuli. All polymer nanotherapeutics were proposed as water-soluble drug delivery systems with a hydrodynamic size below 10 nm ensuring suitability for the parenteral application and preventing opsonization by the reticuloendothelial system. The nanotherapeutics bearing an ester-bound ASA exhibited long-term release of the ASA/salicylic acid mixture, while the nanotherapeutics carrying salicylic acid hydrazide (SAH) ensured the selective release of SAH in the acidic inflammatory environment thanks to the pH-sensitive hydrazone bond between the polymer carrier and SAH. The ASA- and SAH-containing nanotherapeutics inhibited both

cyclooxygenase isoforms and/or the production of pro-inflammatory mediators. Thanks to their favorable design, they can preferentially accumulate in the inflamed tissue, resulting in reduced side effects and lower dosage, and thus more effective and safer treatment.

Highlights

- HPMA-based nanotherapeutics carrying anti-inflammatory drug ASA or SAH effectively reduced pro-inflammatory mediators
- Water-solubility and size up to 10 nm enable parenteral application and preferential accumulation at the inflammation site
- Nanotherapeutics with ASA showed long-term drug release and SAH-based nanotherapeutics showed controlled drug release in the acidic environment
- Several analytical methods were used for detailed drug release experiments and drug decomposition studies

Introduction

Salicylates are known for their therapeutic effects with acetylsalicylic acid (ASA) being the most frequently used drug worldwide[1]. Beyond their analgesic, antipyretic, and anti-inflammatory effects, they are prescribed for the treatment of vascular diseases, in dermatology, in preventing cancer, diabetes, or preeclampsia in pregnant women[2–5]. Their mechanism of action lies in the inhibition of cyclooxygenase 1 and 2 (COX-1, COX-2), which leads to decreased production of prostaglandins and thromboxanes from arachidonic acid, thereby reducing pain, inflammation, swelling, and fever. ASA irreversibly inhibits COX through acetylation and simultaneously interacts noncovalently through its COOH group with the active site of the enzyme. While COX-1 is constitutively expressed in humans[6], the COX-2 isoform was previously thought to be an inducible isoform in pathological conditions, e.g. cancer, atherosclerosis, and inflammation. However, recent studies have detected COX-2 in normal tissue, suggesting a correlation between COX-2 expression and age.[6–8] Moreover, several studies showed that ASA also interferes with the Nuclear factor kappa B (NF-κb) pathway by inhibiting IκB kinase[9,10]. NF-κb pathway regulates genes involved in acute phase inflammatory response, e.g., induces the transcription of nitric oxide synthase (iNOS) and COX-2. Recently, ASA has been shown to affect the production of aspirin-triggered pro-resolving lipid mediators, powerful agents for the resolution of inflammation or cancer[11,12].

Despite the wide use, ASA or salicylic acid (SA) application may cause severe side effects in off-target organs, primarily due to multiple or high dosages. Polymer nanotherapeutics offer many advantages compared to low-molecular-weight drugs, e.g. reduction of the adverse effects and systemic toxicity, improvement of drug pharmacokinetics, drug targeting, etc.[13] Similarly to the Enhanced Permeability and Retention (EPR) effect[14], polymer-based drug delivery systems accumulate in the inflammation sites due to Extravasation through Leaky Vasculature and subsequent Inflammatory cell-mediated Sequestration (ELVIS effect) [15–18]. To prolong the salicylate half-life *in vivo*, achieve sustained release, and thus decrease side effects, several polymer systems bearing SA or ASA were prepared for the treatment of inflammation and cancer, or as biocompatible materials with a wide range of applications[19–23]. SA was polymerized into poly(salicylic acid) or amphiphilic block polymers[21], copolymerized to form salicylic acid-based polyesters[24–26], and directly conjugated to the polymer backbone[27]. ASA-loaded hydrogels[23,28], nanoparticles and membranes[19,29,30], or a series of biocompatible polymers with ester-bonded ASA have also been synthesized and characterized.[31] However, most of these materials are unsuitable for parenteral application and

are unable to accumulate in the site of inflammation through the ELVIS effect. In addition, the direct polymerization of salicylate limits the possibility of modifying the drug release rates or releasing the drug upon specific stimuli. Therefore, the SA release from these systems is often very slow under physiological conditions. In the case of ASA-loaded systems, the release is determined by the degradation of the platform or by simple diffusion and is also difficult to control, with rather rapid diffusion of ASA from the system[30]. Notably, only a few papers discuss the hydrolysis of ASA to SA in their release studies. However, the decomposition of ASA to SA is a well-known process[32], and some of the biological effects of these molecules differ[33].

Hydrophilic biocompatible *N*-2-(hydroxypropyl)methacrylamide (HPMA) copolymers have repeatedly proven to serve as efficient and safe drug carriers capable of the passive accumulation at the site of inflammation and selective release of the drug in the acidic microenvironment of the inflamed tissue[34–36]. Therefore, we aimed to develop fully water-soluble, highly defined nanotherapeutics, specifically polymer conjugates based on HPMA copolymers that release either ASA derivatives or ASA and SA upon specific stimuli, i.e. pH change, to deliver these anti-inflammatory agents to affected inflammatory tissues (see Scheme 1). A series of ASA derivatives and their polymer conjugates were synthesized and characterized, and we focused on their behavior in physiological conditions and *in vitro* evaluation. We also followed up on the issue of ASA hydrolysis to salicylic acid. Moreover, we studied the biological behavior of another molecule, salicyloyl hydrazide (SAH) as a promising anti-inflammatory agent. We anticipate that targeted delivery of these systems may significantly improve the treatment of various inflammatory diseases, e.g. rheumatoid arthritis or cystic fibrosis[37], due to the reduced production of pro-inflammatory cytokines and enhanced biosynthesis of pro-resolving mediators. Thanks to the water solubility of the polymer conjugates and excellent biocompatibility, the systems are appropriate for parenteral application to treat both localized and systemic inflammation. The suitable hydrodynamic size of the polymer carriers enables prolonged circulation *in vivo*, compared to the low-molecular-weight drugs, as well as preferential accumulation in inflamed tissue, where the drug can be released. All these benefits could lead to increased treatment efficacy, reduced side effects, and lower dosage, thereby enhancing treatment outcome and safety, especially in the treatment of chronic inflammation, where multiple doses of anti-inflammatory drugs are usually required.

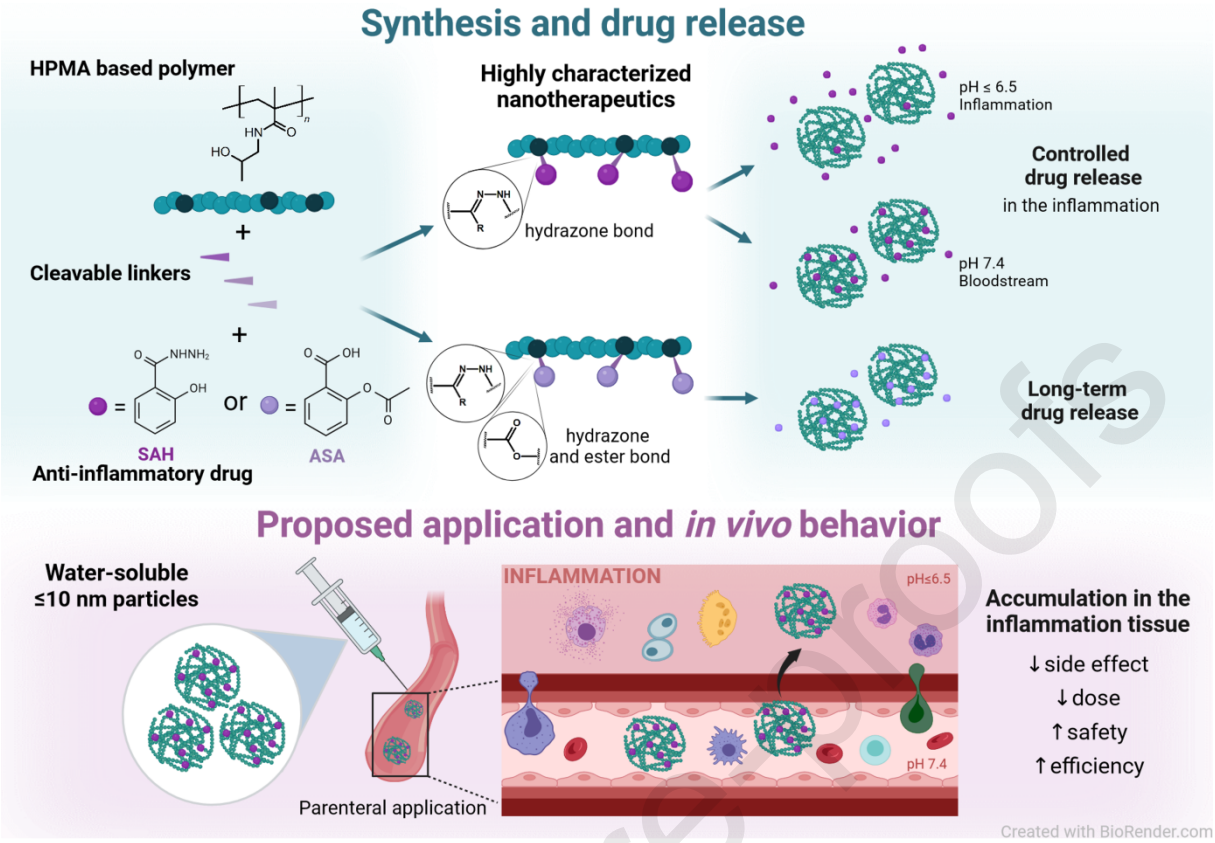

Scheme 1. Schematic description of polymeric nanotherapeutics for the controlled release of ASA and SAH; synthesis, behavior in aqueous solution, drug release, proposed application, and expected fate *in vivo*.

1 Experimental procedures

1.1 Materials

2,2′-Azobisisobutyronitrile (AIBN), *N*-ethylmaleimide, sodium borohydride, 2,4,6-trinitrobenzene-1-sulfonic acid (TNBSA), 4-(4-hydroxyphenyl)-2-butanone (HFB), 4-hydroxy-2-butanone (HB), 4-hydroxybenzaldehyde (HBA), *N*-(3-dimethylaminopropyl)-*N*′-ethylcarbodiimide hydrochloride (EDC·HCl), isopropyl carbodiimide (DIC), 4-(dimethylamino)pyridine (DMAP), acetylsalicylic acid (ASA), salicylic acid (SA), salicyloyl hydrazide (SAH), 4-cyano-4-(thiobenzoylthio)pentanoic acid (ABIC-DTB) and 4,4′-azobis(4-cyanopentanoic acid) (ABIC) were purchased from Sigma-Aldrich. 2,2'-Azobis(4-methoxy-2,4-dimethylvaleronitrile) (V-70) was purchased from Wako Chemicals (USA). *N*-(3-*tert*-butoxycarbonyl-aminopropyl)methacrylamide (APMA-Boc) was purchased from Polysciences, Inc. (PA, USA). 5-Cyclohexyl-5-oxopentanoic acid (COV) was purchased from Rieke Metals (USA). Dichloromethane (DCM), dimethyl sulfoxide (DMSO), *N,N*-

dimethylacetamide (DMA), *tert*-butanol (*t*-BuOH), *N,N*-diisopropylethylamine (DIPEA), Trifluoroacetic acid (TFA) and other common or special chemicals or solvents were purchased from Sigma-Aldrich, Lach-ner, or VWR International (Czech Republic). The solvents were dried and purified by conventional procedures. The other materials were used as received.

The biological measurements were conducted using the following materials: Murine peritoneal macrophage cells RAW 264.7 (American Type Culture Collection, USA), Dulbecco's Modified Eagle Medium (DMEM, Gibco, Ireland), fetal bovine serum (Gibco, Ireland), Penicillin/streptomycin (Gibco, Ireland), lipopolysaccharide (LPS) from *E. coli* serotype 026:B6 (Sigma-Aldrich, Germany), 3-(4,5-dimethylthiazol-2-yl)-2,5-diphenyltetrazolium bromide (MTT, Sigma Aldrich, Germany), Cytotoxicity Detection KitPLUS (Roche, USA), Griess reagent (Sigma, Germany), phenylmethylsulfonyl fluoride (Sigma Aldrich), BCA™ protein assay (Pierce, USA), bovine serum albumin (AppliChem GmbH, Germany), TNF alpha Mouse ELISA Kit (ThermoFisher), murine Immune Interferon γ (IFNγ, Peprotech, USA), COX (ovine) Colorimetric Inhibitor Screening Assay Kit (Cayman Chemical, SpinChem, Czech Republic).

1.2 Synthesis of monomers

***N*-(2-hydroxypropyl) methacrylamide** (HPMA) and ***N′*-[6-(methacryloylamino)-hexanoyl]-hydrazine carboxylic acid tert-butyl ester** (Ma-AH-NHNH-Boc) were prepared according to the previous procedure[38,39].

1.3 Synthesis of functionalized chain transfer agent (CTA)

S-2-cyano-2-propyl-S′-ethyl trithiocarbonate (AIBN-TTC) was synthesized as described by Ishitake et al.[40]

1.4 Synthesis of the ASA derivatives and modified COV

1-cyclohexyl-5-(2-sulfanylidene-1,3-thiazolidin-3-yl)pentane-1,5-dione (COV-TT)

COV (300.0 mg, 1.51 mmol) was dissolved in dry DCM (10 mL) under argon before the addition of 2-thiazoline-2-thiol (270.6 mg, 2.27 mmol), EDC·HCl (435.1 mg, 2.27 mmol), and DMAP (40.0 mg, 0.30 mmol). The reaction was monitored using HPLC and TLC (hexane/ethyl acetate 2/1). After 18 h, the reaction mixture was washed with water (100 mL), 5% $NaHCO_3$ (100 mL), and water (100 mL) and dried with $MgSO_4$. After column chromatography (hexane/ethyl acetate 7/1 to 3/1), the product was isolated in the form of a yellow powder (300.0 mg, 67 %). HPLC purity 99 %. ^{1}H NMR (400 MHz, $CDCl_3$): δ = 4.58 (t, 2 H, J = 7.5 Hz, -

NC*H*$_2$CH$_2$-), 3.30 (t, 2 H, *J* = 7.4 Hz, -NCH$_2$C*H*$_2$-), 3.27 (t, 2 H, *J* = 7.2 Hz, -C*H*$_2$C(O)N-), 2.57 (t, 2 H, *J* = 7.1 Hz, -CHC(O)C*H*$_2$-), 2.39 – 2.28 (m, 1 H, C*H* from cyclohexane), 1.95 (p, 2 H, *J* = 7.3 Hz, -CH$_2$C*H*$_2$CH$_2$-), 1.89 – 1.12 (m, 10 H, 5 × C*H*$_2$ from cyclohexane) ppm. ^{13}C (101 MHz, CDCl3): δ = 213.6 (1 C, -CH*C*(O)CH$_2$-), 201.8 (1 C, -S*C*(S)N-), 174.5 (1 C, -CH$_2$*C*(O)N-), 56.2 (1 C, -N*C*H$_2$CH$_2$-), 51.1 (1 C, -*C*HC(O)-), 39.9 – 25.5 (8 × C, 5 × *C*H$_2$ from cyclohexane, -CHC(O)*C*H$_2$-, -*C*H$_2$C(O)N-, -NCH$_2$*C*H$_2$-), 18.9 (1 C, -CH$_2$*C*H$_2$CH$_2$-) ppm.

(3-oxobutyl)-2-acetoxybenzoate (OAB)

ASA (300.0 mg, 1.7·10^{-3} mol) and DIC (231.0 mg, 1.8·10^{-3} mol) were added to a flask and cooled in an ice bath under argon. After 30 min, HB (175.8 mg, 2.0·10^{-3} mol) dissolved in dry DCM (2.0 mL) and DMAP (3.0 mg, 2.5·10^{-5} mol) were added and the reaction was monitored using HPLC. After 3 h, the reaction mixture was evaporated, re-dissolved in a mixture of methanol (2 mL) and acetonitrile (4 mL), and purified using a FLASH chromatography system. The main product, **OAB,** was isolated in the form of a white solid (131.0 mg, 31 %). HPLC purity 97 %. ^{1}H NMR (400 MHz, DMSO-*d6*): δ = 7.91 – 7.85 (m, 1 H, Ar-6), 7.71 – 7.64 (m, 1 H, Ar-4), 7.44 – 7.36 (m, 1 H, Ar-5), 7.26 – 7.21 (m, 1 H, Ar-3), 4.39 (t, 2 H, *J* = 6.1 Hz, -OC*H*$_2$CH$_2$-), 2.90 (t, 2 H, *J* = 6.1 Hz, -OCH$_2$C*H*$_2$-), 2.27 (s, 3 H, -OC(O)C*H*$_3$), 2.15 (s, 3 H, -CH$_2$C(O)C*H*$_3$) ppm. ^{13}C NMR (101 MHz, DMSO-*d6*): δ = 205.97 (1 C, -CH$_2$*C*(O)CH$_3$), 168.98 (1 C, -O*C*(O)CH$_3$), 163.91 (1 C, Ar-*C*(O)OCH$_2$-), 149.94 (1 C, Ar-2), 134.20–124.05 (4 × C, Ar-3 – Ar-6), 123.02 (1 C, Ar-1), 60.17 (1 C, -O*C*H$_2$CH$_2$-), 41.34 (1 C, -OCH$_2$*C*H$_2$-), 29.93 (1 C, -CH$_2$C(O)*C*H$_3$), 20.67 (1 C, -OC(O)*C*H$_3$) ppm. MS(ESI): m/z calculated for C$_{13}$H$_{14}$O$_5$Na [M+Na]$^+$ 273.07; found 273.00.

(4-formylphenyl)-2-acetoxybenzoate (FAB)

The ASA derivative **FAB** was prepared using the same procedure as that for the derivative **OAB**. ASA (150.0 mg, 8.3·10^{-4} mol), DIC (115.5 mg, 9.2·10^{-4} mol), HBA (122.1 mg, 1.0·10^{-3} mol), and DMAP (1.5 mg, 1.3·10^{-5} mol) were mixed in dry DCM (5.0 mL) under cooling and an argon atmosphere. The main product, **FAB**, was isolated by FLASH chromatography as a white solid (108.0 mg, 46 %). HPLC purity 98 %. ^{1}H NMR (400 MHz, DMSO-*d6*): δ = 10.04 (s, 1 H, -C*H*O), 8.22 – 8.17 (m, 1 H, Ar-6), 8.07 – 8.00 (m, 2 H, Ar-2‘, Ar-6‘), 7.84 – 7.77 (m, 1 H, Ar-4), 7.55 – 7.47 (m, 3 H, Ar-5, Ar-3‘, Ar-5‘), 7.37 – 7.32 (m, 1 H, Ar-3), 2.26 (s, 3 H, -OC(O)C*H*$_3$) ppm. ^{13}C NMR (101 MHz, DMSO-*d6*): δ = 191.99 (1 C, *C*HO), 169.41 (1 C, -O*C*(O)CH$_3$), 162.03 (1 C, Ar-*C*(O)O-Ar), 154.64 (1 C, Ar-1‘), 150.67 (1 C, Ar-2), 135.33–

121.84 (10 × C, Ar-1, Ar-3 – Ar-6, Ar-2‘ – Ar-6‘), 20.73 (1 C, -OC(O)*C*H$_3$) ppm. MS(MALDI-TOF): m/z calculated for $C_{16}H_{12}O_5Na$ $[M+Na]^+$ 307.058; actual 307.087.

[4-(3-oxobutyl)phenyl]-2-acetoxybenzoate (OPAB)

The ASA derivative **OPAB** was prepared according to the procedure for **OAB**. ASA (300.0 mg, $1.7\cdot10^{-3}$ mol), DIC (231.0 mg, $1.8\cdot10^{-3}$ mol), HFB (328.2 mg, $6.7\cdot10^{-4}$ mol), and DMAP (3.0 mg, $2.5\cdot10^{-5}$ mol) were mixed in dry DCM (5.0 mL) under cooling and an argon atmosphere. The main product, **OPAB,** was isolated by FLASH chromatography in the form of a white solid (226.0 mg, 42 %). HPLC purity 100 %. ^{1}H NMR (400 MHz, DMSO-*d6*): δ = 8.17 – 8.8.11 (m, 1 H, Ar-6), 7.81 – 7.73 (m, 1 H, Ar-4), 7.53 – 7.46 (m, 1 H, Ar-5), 7.34 – 7.27 (m, 3 H, Ar-3, Ar-3‘, Ar-5‘), 7.14 – 7.08 (m, 2 H, Ar-2‘, Ar-6‘), 2.82 – 2.78 (m, 4 H, -C*H$_2$*C*H$_2$*C(O)-), 2.24 (s, 3 H, -OC(O)C*H$_3$*), 2.10 (s, 3 H, -CH$_2$C(O)C*H$_3$*) ppm. ^{13}C NMR (101 MHz, DMSO-*d6*): δ = 207.52 (1 C, -CH$_2$*C*(O)CH$_3$), 169.31 (1 C, -O*C*(O)CH$_3$), 162.87 (1 C, Ar-*C*(O)O-Ar), 150.27–148.27 (2 × C, Ar-2, Ar-1‘), 139.40–121.47 (10 × C, Ar-1, Ar-3 – Ar-6, Ar-2‘ – Ar-6‘), 44.08 (1 C, Ar-CH$_2$*C*H$_2$-), 29.63–28.05 (2 × C, Ar-*C*H$_2$CH$_2$C(O)*C*H$_3$), 20.47 (1 C, -OC(O)*C*H$_3$) ppm. MS(ESI): m/z calculated for $C_{19}H_{18}O_5Na$ $[M+Na]^+$ 349.10; found 349.08.

1.5 Synthesis of polymer precursors

The HPMA copolymer P1 with hydrazide groups

The precursor **P1** was synthesized by Reversible Addition−Fragmentation chain-Transfer (RAFT) copolymerization of HPMA and MA-AH-NHNH-Boc using a chain transfer agent AIBN-TTC and an initiator V-70, followed by end chain-group removal and hydrazide groups deprotection.

The polymerization was performed as follows: the molar ratio of monomer units:CTA:initiator was 400:2:1 and the molar ratio of HPMA:MA-AH-NHNH-Boc was 92:8. Monomer HPMA (1.00 g, 6.98 mmol) was dissolved in *t*-BuOH (9.76 ml) in a polymerization ampoule before the addition of Ma-AH-NH-NH-Boc (190.0 mg, 0.61 mmol), AIBN-TTC (7.8 mg, 0.038 mmol) and V-70 (5.9 mg, 0.019 mmol) dissolved in dry DMSO (1.08 ml). The mixture was bubbled with argon for 10 minutes, sealed and the polymerization was performed at 30°C for 72 h. The final copolymer was isolated by precipitation into a mixture of acetone:diethyl ether (3:1, 400 ml), dried under a vacuum, and purified by re-precipitation from methanol (10 ml) into the mixture of acetone:diethyl ether (3:1, 400 ml). The yield was 1.0 g (84 %).

The trithiocarbonate (TTC) ω-end groups were removed by a method described by Perrier[41] using AIBN followed by a subsequent reduction of remaining TTC[42]. Briefly, the copolymer (1.0 g) was dissolved in dry DMSO (6.70 ml), AIBN (200 mg) was added, and the mixture was bubbled with argon and heated to 80°C for 3 h in an ampoule. The copolymer was precipitated into ethyl acetate (200 ml), dried under a vacuum, and subsequently purified by re-precipitation from methanol (6.6 ml) into ethyl acetate (200 ml). After drying in a vacuum, the copolymer (811 mg) was dissolved in dry methanol (7 ml), sodium borohydride (6.0 mg) was added in portions, and after 10 min, the *N*-ethylmaleimide (22.0 mg) was added in portions. After 30 min of stirring, the copolymer was purified on a Sephadex LH-20 column in methanol, concentrated under a vacuum, dissolved in water, and freeze-dried (750 mg).

Tert-butoxycarbonyl (Boc)-protected hydrazide groups of the copolymer were deprotected using a method developed in our group[43]. The HPMA copolymer (750 mg) was dissolved in distilled water (20 mL) and heated to 100°C for 1 h in a sealed ampoule. Subsequently, the copolymer was freeze-dried and the content of hydrazide groups was determined using TNBSA assay[43].

The HPMA copolymer P2 with amine groups

The precursor **P2** was synthesized by RAFT copolymerization of HPMA and APMA-Boc using a chain transfer agent ABIC-DTB and an initiator ABIC, followed by end chain-group removal and deprotection of primary amine groups.

The polymerization was performed as follows: the molar ratio of monomer units:CTA:initiator was 350:2:1 and the molar ratio of HPMA:APMA-Boc was 94:6. Monomer HPMA (2.02 g, 14.10 mmol) was dissolved in MiliQ water (10.0 ml) in a polymerization ampoule, before the addition of APMA-Boc (206.9 mg, 0.86 mmol), ABIC-DTB (25.2 mg, 0.090 mmol) and ABIC (12.0 mg, 0.043 mmol) dissolved in dioxane (5.00 ml). The mixture was bubbled with argon for 10 minutes, sealed, and the polymerization was performed at 70°C for 7 h. The final copolymer was isolated by precipitation into acetone (400 ml), dried under a vacuum, and purified by re-precipitation from methanol (20 ml) into the mixture of the acetone:diethyl ether (3:1, 400 ml). The yield was 1.8 g (79 %).

The dithiobenzoate ω-end groups were removed by the same method described above for **P1**. Protecting Boc groups were removed by dissolving the polymer in the mixture TFA/triisopropylsilane/water 95/2.5/2.5 (vol. %) at a polymer solution concentration of 10% (w/v) and precipitated into diethyl ether. The precipitate was dissolved in MiliQ water, the pH was adjusted with NaOH to 7-8, and the copolymer was then isolated by gel filtration on a

Sephadex G25 column in water and freeze-dried (1.32 g). The content of the amine groups was determined using TNBSA assay[43].

The HPMA copolymer P3 with keto groups

The copolymer **P3** was prepared from the HPMA copolymer **P2** containing amine groups and COV-TT as follows: the copolymer **P2** (800.0 mg, 5.0 mol% of amines) was dissolved in DMA (10 mL) and COV-TT (157.0 mg, 2-fold molar excess to the amine groups) in DMA (3 mL) and DIPEA (0.092 mL) were added. The reaction was monitored using HPLC. After 2 h, acetic anhydride (0.025 mL) and DIPEA (0.046 mL) in DMA (0.5 mL) were added to block possible remaining amines. After 0.5 h, the copolymer was purified using a Sephadex LH20 column in methanol, concentrated, isolated by precipitation into ethyl acetate (200 mL), and dried under a vacuum (700.0 mg).

1.6 Synthesis of polymer conjugates

The copolymers **P1**, or **P3**, were dissolved in dry DMSO (for **P1**), or methanol (for **P3**). Afterward, the ASA derivative (for **P1**) or SAH (for **P3**) and acetic acid were added. The reaction was monitored using HPLC. After 18 h, the polymer conjugate was purified on a Sephadex column in methanol, concentrated, precipitated into ethyl acetate, and dried under a vacuum. The conjugates were characterized using SEC, DLS (Tab. 2), and NMR (Fig. S1).

Polymer conjugate with (3-oxobutyl)-2 -acetoxybenzoate (P1-OAB)

Copolymer **P1** (250.0 mg) was dissolved in dry DMSO (2.0 mL), and **OAB** (18.8 mg, 4.5 mol% - calculated to monomer unit) and acetic acid (0.068 mL) were added. The **P1-OAB** was isolated as a white powder (202.0 mg).

Polymer conjugate with (4-formylphenyl)-2 -acetoxybenzoate (P1-FAB)

Copolymer **P1** (250.0 mg) was dissolved in dry DMSO (2.0 mL), and **FAB** (21.3 mg, 4.5 mol% - calculated to monomer unit) and acetic acid (0.068 mL) were added. **The P1-FAB** was isolated as a white powder (245.0 mg).

Polymer conjugate with [4-(3-oxobutyl)phenyl]-2 -acetoxybenzoate (P1-OPAB)

Copolymer **P1** (250.0 mg) was dissolved in dry DMSO (2.0 mL), and **OPAB** (24.5 mg, 4.5 mol% - calculated to monomer unit) and acetic acid (0.068 mL) were added. The **P1-OPAB** was isolated as a white powder (235.0 mg).

Polymer conjugate with salicyloyl hydrazide (P3-SAH)

Copolymer **P3** (660.0 mg) was dissolved in dry methanol (7.0 mL), and SAH (33.0 mg, 5 mol% - calculated to monomer unit) and acetic acid (0.8 mL) were added. The **P3-SAH** was isolated as a white powder (620.0 mg).

1.7 Drug release and stability measurements

Hydrolytic stability of ASA derivatives

The solutions of ASA derivatives (OAB, OPAB, FAB) in DMSO (100 mg·mL^{-1}) were placed into Eppendorf vials containing phosphate buffers (0.15 M, pH 7.4 or 5.0) to obtain the final concentration of 1 mg·mL^{-1} of ASA derivative and 0.5% v/v DMSO. The suspensions of ASA derivatives in buffers were incubated under shaking on a Thermometer comfort (500 rpm, Eppendorf) at 37°C. At 0, 1, 3, 5, 20, and 24 h, samples were diluted with acetonitrile to a concentration of 0.125 mg·mL^{-1}, centrifuged, and the supernatants were analyzed by HPLC.

Release of SAH and ASA derivatives from polymer conjugates

Extraction method: Release of ASA derivatives and SAH from polymer conjugates P1-FAB, P1-OPAB, and P3-SAH was performed in phosphate buffers (0.15 M, pH 7.4 or 5.0) at 37°C in triplicate. Solutions of P1-FAB and P1-OPAB (200 μL, 1 mg·mL^{-1}) were incubated under shaking on a Thermometer comfort (500 rpm, Eppendorf) and samples were collected at selected time points and washed with dichloromethane (0.5 mL). After 10 min of extraction, the organic phase (0.4 mL) was evaporated, resuspended in methanol (100 μL), and analyzed by HPLC (Chromolith C-18 column). The amount of released drug was determined using a calibration curve at 220 nm. The solution of P3-SAH (200 μL, 5 mg·mL^{-1}) was incubated under shaking on a Thermometer comfort (500 rpm, Eppendorf) and samples were washed with DCM (0.5 mL) at selected time points. After 10 min of extraction, the organic phase (0.4 mL) was evaporated, resuspended in methanol (80 μL), and diluted with MiliQ water (20 μL). The amount of released drug was determined using HPLC (Luna column) and a calibration curve at 220 nm. The area of the peaks was multiplied with a coefficient of extraction 1.8 (experimentally determined) since SAH is extracted into dichloromethane from 55%. NMR spectroscopy was used to determine the amount of the drug attached to the polymer carrier (for P1-FAB, P1-OPAB, and P3-SAH), and this quantity was used as a maximum released drug (100% release) to construct the release curve.

Capillary electrophoresis (CE) method: The release of ASA/SA from P1-FAB and SAH from P3-SAH were also monitored with CE. Polymer conjugates P1-FAB and P3-SAH were dissolved in phosphate-citrate buffers (0.15 M, pH 5.0 or 7.4) to the concentration of 5 mg·mL^{-1} and incubated at 37°C. After 0.25, 1, 2, 4, 6, 20, and 24 h, 40 µL of the polymer solution was pipetted into a CE sample vial and 4 µL of sodium benzene sulfonate solution (1 mg·mL^{-1}) was added as an internal standard. The sample was injected into the CE system without any further treatment. All samples were prepared and measured in triplicate. Calibration standards were prepared (5, 10, 20, 50, 100, and 200 µg·mL^{-1}) and contained 5 mg·mL^{-1} polymer precursor (without the drugs) to match the matrix with the measured samples. All calibration samples contained benzene sulfonate as an internal standard. The calibration curve was constructed by plotting the analyte and benzene sulfonate peak area ratio as a function of analyte concentration (R2 ≥ 0.9998). The quality control sample was prepared at the 50 µg·mL^{-1} concentration of analytes and measured after every 3 runs.

1.8 Physico-chemical characterization and purification methods

Nuclear magnetic resonance (NMR) spectroscopy: Structures of the CTA, ASA derivatives, COV-TT, monomers, polymer precursors, and polymer-drug conjugates were confirmed with an NMR Bruker Avance Neo 400 spectrometer operating at 400.13 MHz (^{1}H) and 100.61 MHz (^{13}C) using DMSO-*d6* or $CDCl_3$ with the following settings: π/2 pulse width 16.5 µs, relaxation delay 10 s, spectral width 6 kHz, acquisition time 3.28 s (^{1}H), 1.22 s (^{13}C), 16-64 scans (^{1}H), 300-400 scans (^{13}C). NMR spectra were evaluated in Software Topspin version 4.0.9 and all samples were measured in 5 mm NMR tubes at a concentration of around 10 mg·mL^{-1}. The numbering of atoms of ASA derivatives for NMR spectra transcription was performed as shown in Figure S2. Letters "I" and "I′" in Figure S1 (NMR of polymer conjugates) indicate unassigned or overlapped signals.

Size exclusion chromatography (SEC): Molecular weights (M_w, M_n) and dispersities ($Đ$) of the HPMA polymer precursors and polymer conjugates were determined using a Shimadzu HPLC system equipped with an SEC column (TSKgel Super SW3000, 300 × 4.6 mm) in methanol/0.3M sodium acetate buffer (4/1, v/v; pH 6.5; flow 0.5 mL·min^{-1}), refractive index detector Optilab-rEX (RI), multiangle light scattering (MALS) detector (DAWN HELEOS II, Wyatt Technology Co., USA) and SPD-M20A photodiode array detector (Shimadzu, Japan). Astra software was used for the evaluation of the samples (refractive index increment dn/dc = 0.167 mL·g^{-1}).

Purification of copolymers: The HPMA copolymers and polymer-drug conjugates were purified by precipitation or with Sephadex columns (LH-20, G25) equipped with a UV flow detector (Azura UVD 2.1S, Knauer, Germany). The fractions were collected at 230 nm.

Light scattering: Dynamic light scattering (DLS; Nano-ZS, Model ZEN3600, Malvern, UK) was used for the determination of the hydrodynamic diameter (D_h) of the samples. The measurements were performed in PBS buffer using a scattering angle of 173° and laser with λ = 632.8 nm. The samples were prepared at a concentration of 5 mg·mL^{-1} and filtered through a 0.2 μm PVDF filter.

UV-Vis spectrometry: The content of hydrazide and amine groups was determined by UV-Vis spectrophotometry (Specord205 ST, Analytic Jena AG, Germany) using the TNBSA assay[43].

High-performance liquid chromatography (HPLC) measurement: HPLC analyses of low-molecular-weight compounds, monitoring of reactions, and measurements of drug release were performed on an HPLC chromatograph (Shimadzu, LC-20AD) using reverse-phase columns (Chromolith Performance RP-18e 100 × 4.6 mm, Merck Millipore or Luna Omega 5 μm Polar C18 100 × 4.6 mm, Phenomenex) with diode array detector (Shimadzu, SPD-M20A), using a mobile phase water/acetonitrile (for drug attachment monitoring) or water/acetonitrile/0.1% TFA (basic analysis) with a gradient of 5–95% v/v acetonitrile at a flow rate of 4 or 5 mL·min^{-1}.

Mass spectrometry (MS): The molecular mass of the low-molecular-weight compounds was determined by mass spectrometry performed on an LCQ Fleet mass analyzer with electrospray ionization (MS ESI; Thermo Fisher Scientific, Inc., MA, USA) in methanol, or using Matrix Assisted Laser Desorption/Ionization–Time Of Flight (MALDI–TOF) mass spectrometry. MALDI-TOF mass spectra were acquired with the UltrafleXtreme TOF – TOF mass spectrometer (Bruker Daltonics, Bremen, Germany) equipped with a 2000 Hz smartbeam-II laser (355 nm) using the positive ion reflectron mode. Panoramic pulsed ion extraction and external calibration were used for molecular weight assignment. The dried droplet method was used, in which the solutions of the sample (10 mg·mL^{-1}) and matrix 2,5-dihydroxybenzoic acid (Sigma–Aldrich, 98%, 20 mg·mL^{-1}) in methanol were mixed in the volume ratio 4:20. Subsequently, 1 μL of the mixture was deposited on the ground-steel target and dried at ambient temperature.

Capillary electrophoresis (CE): The concentrations of SA, ASA, and SAH released from polymer conjugates P1-FAB and P3-SAH were monitored on an Agilent 7100 CE system (Agilent Technologies, Waldbronn, Germany). Unmodified fused silica capillary, 50 μm i.d., 375 μm o.d., 50.0 cm total, and 41.5 cm effective length (Polymicro Technologies, Phoenix, USA) was thermostatted at 25°C. Samples were injected using a pressure of 5 kPa for 5 s. The separation voltage was 30 kV (current approx. 48 μA). The diode array detector was set at the 200 nm wavelength. Sodium tetraborate (20 mM, pH = 9.2) was used as a background electrolyte. Before each run, the capillary was rinsed for 2 min with 1 M NaOH, 1 min with water, and 2 min with background electrolyte using a pressure of approx. 93 kPa. OpenLab software was used for data acquisition and analysis. Migration times of SAH, ASA, SA, and benzene sulfonate (internal standard) were 3.1, 3.2, 3.8, and 4.1 minutes, respectively.

Thin layer chromatography (TLC): TLC on silica gel 60 F254-coated aluminum sheets (Merck, Germany) was used with UV detection at λ = 254 nm to monitor the reactions and product purity control.

Purification of low-molecular-weight compounds: The purification of low-molecular-weight compounds was performed using column chromatography on normal phase (Silica gel 60, Merck, Germany) or FLASH chromatographic system (PrepChrom C-700) equipped with a Chromolith Performance RP-18e column (100 × 25 mm, Merck Millipore) using a mobile phase of water/acetonitrile with a gradient of 5–95% v/v acetonitrile at a flow rate of 60 mL·min^{-1}.

1.9 Cell culture

Murine peritoneal macrophage cells RAW 264.7 were cultured in DMEM, supplemented with 10% of fetal bovine serum, 100 U·mL^{-1} of penicillin, and 100 μg·mL^{-1} of streptomycin. Cells were cultured at 37°C in a humidified incubator with an atmosphere of 5% CO_2 and 95% air.[44]

1.10 Cell treatment

The cells were seeded (2.5 × 10^5 cells/well) in a 24-well culture plate and left to adhere overnight. The culture medium was changed and the cells were pre-treated with the compounds for 60 min. The stock solutions were prepared by dissolving the compounds in PBS (polymer conjugates) or DMSO (low-molecular-weight compounds). The concentrations of active molecules were 0.5, 1.0, and 1.5 mM, and the drug-free copolymer precursor was 5.63 and 3.76 mg·mL^{-1} (equal to the mass concentration of polymer in conjugates). The model activator LPS (25 ng·mL^{-1}) was added after pre-treatment and cells were incubated for 24 h.

Acute cytotoxicity

The potential acute cytotoxicity of compounds was evaluated by the measurement of lactate dehydrogenase (LDH) release from the damaged cells using the Cytotoxicity Detection KitPLUS according to the manufacturer's instructions. Culture media was mixed with the working solution and incubated at room temperature before the absorbance was measured at 490 nm using a SPECTRA Sunrise microplate reader (Tecan, Switzerland).

MTT assay

The MTT assay was performed to assess the metabolic activity of live RAW 264.7 cells. 10 µl of MTT solution in PBS (2.5 $mg \cdot mL^{-1}$) was added to the wells and incubated for 4 h. The culture media was aspirated and 300 µl of 10% Triton-X-100 in 0.1M HCl was added per well. The plate was incubated on a shaker at room temperature for 15 min and then the absorbance was measured at 570 nm.

Determination of protein concentration

RAW 264.7 cells were gently washed with cold PBS and lysed using a lysis buffer (1% sodium dodecyl sulfate; 100 mM Tris, pH 7.4; 10% glycerol), phenylmethylsulfonyl fluoride (0.17 $mg \cdot mL^{-1}$) as protease inhibitor was added just before use. The protein concentration of the cell lysates was determined by a BCA™ protein assay using bovine serum albumin as a standard according to the manufacturer's instructions. The absorbance was measured at 562 nm using a SPECTRA Sunrise microplate reader.

Griess assay

The inhibition of nitric oxide (NO) production was determined indirectly by measurement of nitrites in the culture media using Griess reagent. The culture media was mixed 1:1 with Griess reagent and incubated at room temperature for 15 min before the absorbance was measured at 540 nm.

1.11 Inhibition activity of low-molecular-weight compounds and their polymer conjugates to COX

The inhibitory activity of SA, ASA, SAH, FAB, HBA, P1-FAB, and P3-SAH and their polymer precursors (P1 and P3) on COX-1 and COX-2 was determined using a COX (ovine) Colorimetric Inhibitor Screening Assay Kit according to the manufacturer's instructions. Samples (final concentrations 1.5 mM, 1.0 mM, and 0.5 mM represent the concentrations of active molecules, i.e. ASA or SAH in the samples) were dissolved in DMSO and added to the mixture of assay buffer, hemin, colorimetric substrate solution, arachidonic acid, and COX-1

or COX-2 enzyme. P1-FAB and P3-SAH were tested either freshly dissolved or dissolved, diluted in assay buffer, and preincubated for 24 (P3-SAH) or 72 (P1-FAB) hours. Untreated wells with uninhibited COX-1 and COX-2 activity were used as controls. Absorbance at 590 nm was measured on BioTek Synergy H1 Microplate Reader kinetically for 10 minutes and the inhibition was calculated from the linear portion of the kinetic curve.

1.12 Tumor necrosis factor α (TNF-α) production assessment by ELISA

TNF-α produced by the macrophages was measured by ELISA according to the manufacturer's instructions. Briefly, 1×10^4 cells were incubated in 96 well plates in DMEM media. Half of the plate (6 columns) was stimulated with LPS (25 ng·mL^{-1}), as described above, and the other half with LPS (25 ng·mL^{-1}) plus IFNγ (25 ng·mL^{-1}). One column was used as a control, one as the polymer control (P1), and three for different concentrations of the P1-FAB (0.5, 1.0, 1.5 mM – corresponding to the concentration of ASA in the sample). The cells were incubated for 24 h. Then, the plates were centrifuged briefly and 50 µl of each supernatant was added to the ELISA plate for murine TNF-α.

1.13 Statistical analysis

Statistical evaluation of the results was conducted in GraphPad Prism5 and Prism8 software. All data are presented as the mean of two to four experiments and error bars indicate the standard error mean (SEM), *P <0.05, **P <0.01, ***P <0.001.

Results and discussion

2.1 Synthesis of polymer precursors

The polymer precursors **P1** and **P2** were prepared by controlled radical RAFT polymerization using trithiocarbonate- (**P1**) and dithiobenzoate-based (**P2**) chain transfer agents (Scheme 3). As expected, all polymers showed low dispersity. The removal of CTA and Boc deprotection did not change the precursor's dispersity or their molecular weights. The copolymer **P1** containing hydrazide groups was used to attach ASA derivatives containing oxo- groups. The copolymer **P2** containing deprotected amine groups was modified with COV-TT to prepare copolymer **P3** with oxo- groups along the polymer chain enabling attachment of SAH. COV linker was selected according to our previous study.[45] Quantitative attachment of the COV linker to the copolymer **P2** was confirmed by NMR measurement. The characteristics of the polymers are summarized in Table 1. All the polymer precursors had molecular weights that enabled prolonged bloodstream circulation and a sufficient quantity of functional groups for attachment of pharmaceutically active molecules. Moreover, the precise setting of the molecular weight enables the elimination of the precursors after fulfilling its role via glomerular filtration.

Table 1. Characteristics of HPMA copolymer precursors

HPMA polymer	Monomer: CTA:initiator ratio	M_n (g mol^{-1})	M_w (g mol^{-1})	$Đ$	Amine groups (mol %)[a]	Hydrazide groups (mol %)[a]	D_h (nm)[b]
P1	400:2:1	24,200	26,600	1.1	---	6.8	5.4±0.1
P2	350:2:1	22,300	23,500	1.1	5.0	---	4.6±0.2
P3	---	24,800	28,100	1.1	---	---	5.8±0.3

[a]After Boc deprotection, determined by TNBSA

[b]Determined using DLS; measured in PBS; number mean

2.2 Synthesis of ASA derivatives

ASA was esterified with various hydroxyl linkers containing keto/aldehyde groups to introduce functional groups for attachment to the polymer via a pH-sensitive hydrazone bond. The structure of the linkers varied to obtain diverse drug release rates from the polymer backbone. Moreover, the second aim was to find a derivative with suitable stability of the ester bond

between ASA and the linker to ensure the release of free ASA molecule, and thus keep its function in COX inhibition through the carboxylic group. The linkers HB, HBA and HFB were used for the synthesis of ASA derivatives (3-oxobutyl)-2-acetoxybenzoate (**OAB**), (4-formylphenyl)-2-acetoxybenzoate (**FAB**) and [4-(3-oxobutyl)phenyl]-2-acetoxybenzoate (**OPAB**), respectively (Scheme 2). The **OAB** and **OPAB** are newly synthesized compounds, while **FAB** has already been published.[46] The ester was formed by Steglich esterification with DIC, or EDC·HCl as a carbodiimide coupling agent and DMAP as a catalyst. Firstly, the reaction conditions were optimized due to the deacetylation of ASA in the reaction mixture and the formation of numerous side products. The effect of temperature, carbodiimide type, and amount of DMAP was evaluated similarly to Park et al.[47] While the temperature and DMAP amount were crucial for the ASA stability, the type of selected carbodiimide negligibly impacted side product formation. The cooling of the reaction mixture to 0-4°C during ASA activation suppressed the deacetylation, and thus side product formation. The most important parameter influencing the product and side product formation was the amount of DMAP. Without DMAP, the reaction did not proceed as expected, and only the activated form of ASA was observed. The presence of 1.0 mol % of DMAP led to low yields, while the use of 4.0 mol% of DMAP catalyzed the deacetylation of ASA due to the basicity of the DMAP molecule. Finally, 1.5 mol % of DMAP was selected since it gave sufficient yields with less side product formation.

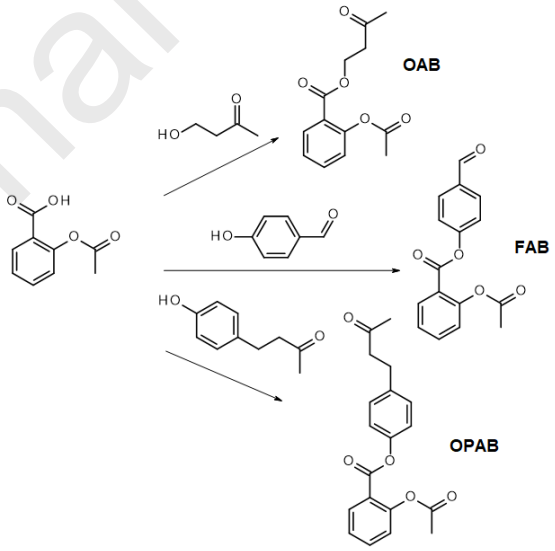

Scheme 2. Synthesis of ASA derivatives (OAB, FAB, OPAB) – reaction conditions: carbodiimide, DMAP, DCM.

2.3 Polymer conjugates synthesis

ASA derivatives **OAB**, **FAB,** and **OPAB** were attached to copolymer **P1** forming a pH-sensitive hydrazone bond enabling release in the acidic environment of inflamed tissue or cell lysosomes. The conjugate synthesis was performed in dry DMSO to prevent the hydrolysis of ester bonds in derivatives. For **FAB** and **OPAB**, the corresponding conjugates **P1-FAB** and **P1-OPAB** were prepared with a satisfactory amount of the bound derivative (Scheme 3, Table 2, Fig. S1). However, the **OAB** repeatedly showed lower binding capacity to **P1** with a maximum content of 3.6 mol %, even with the abundance (8 mol %) of **OAB** in the reaction. Moreover, due to wide dispersity, the resulting **P1-OAB** did not meet the quality criteria (Table 2). The NMR spectrum of **P1-OAB** showing no free hydrazide groups suggested that the ester bond in **OAB** was cleaved during the attachment or purification, and the part of the hydrazide group is occupied only with the linker HB. The polymer conjugate **P3-SAH** was prepared by attaching SAH via its hydrazide group to the keto group of **P3** precursor in methanol. Importantly, the attachment of ASA derivatives **FAB** and **OPAB**, or SAH did not significantly change the molecular weight and dispersity of the conjugates. Besides **P1-OAB**, all the conjugates had proper characteristics for the following biological study.

Table 2. Physico-chemical characteristics of the polymer conjugates

Conjugate	M_n (g mol^{-1})	M_w (g mol^{-1})	$Đ$	Content of drug (mol %/wt %)[a]	Drug attachment efficacy (%)	D_h (nm)[b]
P1-OAB	31,200	49,300	1.5	3.6/5.9	45	---*
P1-FAB	25,900	27,500	1.1	4.4/8.0	97	6.6±0.4
P1-OPAB	26,500	29,100	1.1	4.4/9.1	97	6.7±0.2
P3-SAH	26,300	29,000	1.1	4.3/4.3	86	6.2±0.3

[a]Determined by NMR; corresponds to the content of OAB, FAB, OPAB, and SAH in the polymer conjugates

[b]Determined using DLS; measured in PBS; number mean

*Not determined because of sample quality

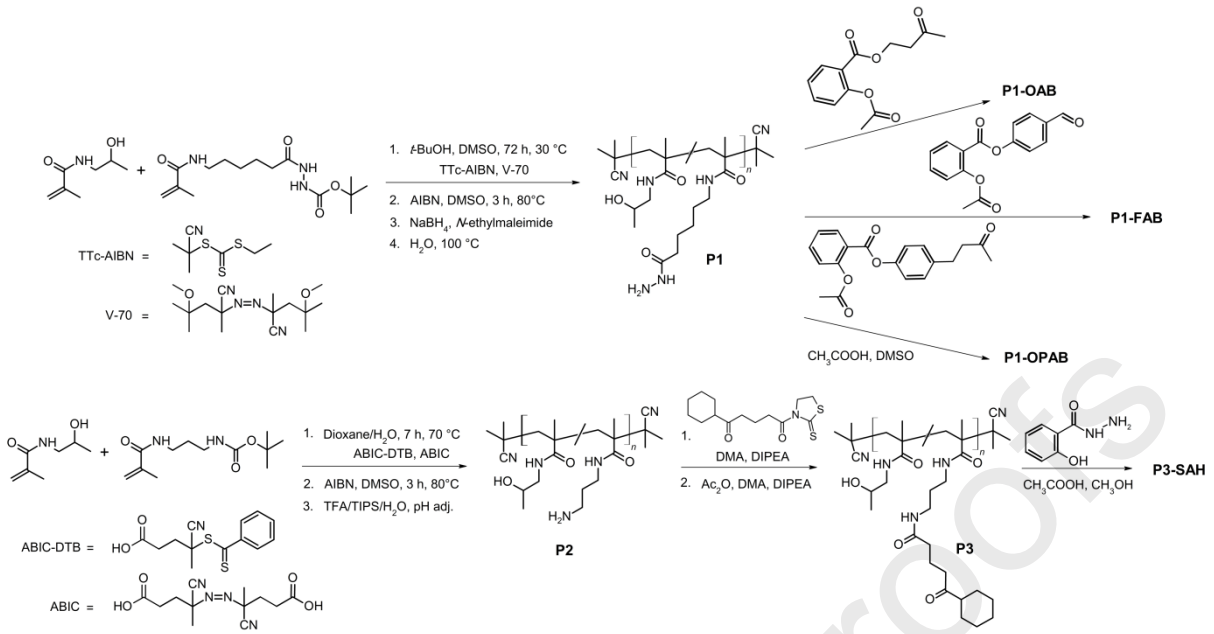

Scheme 3. Synthesis of polymer precursors **P1-P3** and polymer conjugates

2.4 Stability of the ASA derivatives

The stability of the ASA derivatives was assessed in buffers at pH 7.4 and 5.0 (Fig. 1A). As expected for the ester-based derivatives, the derivatives were more stable at pH 5.0 but **OAB** showed low stability at both pHs, with most of the **OAB** derivative decomposed within 4 h at pH 7.4 and around 40% within 24 h at pH 5.0. This poor stability may explain why **P1-OAB** contained an insufficient amount of **OAB**. Thus, we excluded it from further experiments since its rapid decomposition at blood pH would complicate the conjugate application and hinder the conjugate accumulation in inflamed tissues. **FAB** and **OPAB** showed quite good stability at both pHs but ASA and SA were detected in both cases. Derivative **FAB** released 3% of ASA and 4% of SA at pH 7.4 within 24 h, and 1% of ASA was detected at pH 5 within 24 h (Fig. 1B). Derivative **OPAB** released traces of ASA and SA (under 1%) but a small amount of **OPAB** without acetyl was observed, mainly at pH 7.4. The products of the decomposed derivatives are shown in Scheme 4.

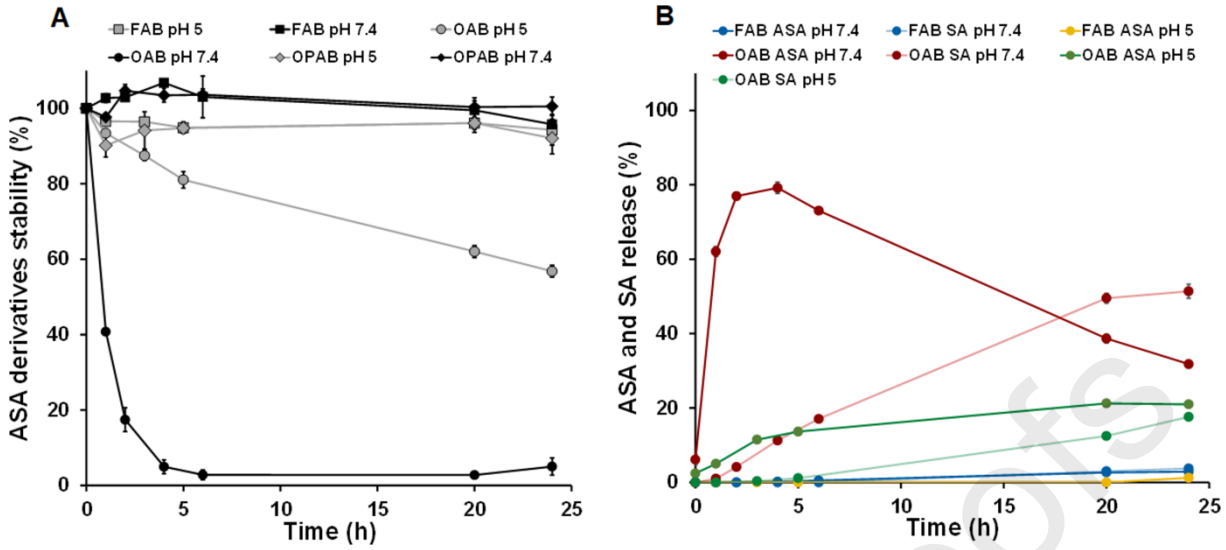

Figure 1. A Stability of ASA derivatives OAB, FAB, and OPAB; **B** ASA and SA release from the ASA derivatives OAB, FAB, and OPAB (37°C, phosphate buffers pH 7.4 and 5.0).

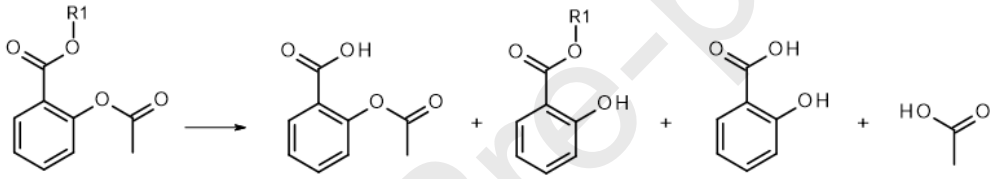

Scheme 4. Decomposition products of ASA derivatives during stability measurement (37°C, phosphate buffers, pH 7.4 and 5.0).

2.5 Release of SAH and ASA derivatives from the polymer conjugates

Release of **OAB** from **P1-OAB** conjugate was not performed due to the low stability of the **OAB** derivative and poor quality of the **P1-OAB** (chapter 2.3 and 2.4). **OPAB** showed a satisfactory release rate from the conjugate **P1-OPAB** (Fig. 2A), with approximately 55% released **OPAB** within 24 h at pH 5.0. Surprisingly, 20% of the derivate was released rapidly within 5 h at pH 7.4. However, the curve started to stagnate after 5 h, which could be ascribed to the slight decomposition of **OPAB** to its deacetylated form at pH 7.4. At pH 5.0, only a small amount of deacetylated **OPAB** was observed. After release from the polymer, it is expected that the **OPAB** will be hydrolyzed *in vivo* to ASA/SA after a longer time or due to enzyme action.

In contrast, the **FAB** derivative showed a slow release rate from **P1-FAB** at both pHs (Fig. 2A), due to the stabilization of the hydrazone bond by the conjugation with aromatic double bonds of **FAB**.[48] However, ASA and SA were probably also released due to the slight instability of the **FAB** derivative (see chapter 2.4.). Unfortunately, the quantitative extraction of ASA and

SA into the dichloromethane phase was impossible; thus, other release methods, such as dialysis, NMR measurement, and capillary electrophoresis (CE), were employed to detect the release of ASA as a key compound. Too high dilution of ASA outside of the dialysis bag and relatively low content of ASA (5.1 wt %) prevented precise quantification of the released ASA by dialysis. NMR measurement showed slight changes in the spectrum after 24 h, but the quantification was impossible because of overlapping peaks (data not shown). Interestingly, the most accurate results were obtained by CE, a useful tool for the release measurement of mostly hydrophilic drugs migrating in an electric field.[49] CE enabled the quantification of the released ASA from the **P1-FAB** conjugate and the ASA/SA ratio (Fig. 2B). At pH 5, only 0.5% of SA was released within 24 h, while ASA was not detected, whereas 7% of SA and up to 2% of ASA were released at pH 7.4 within 24 h. This observation corresponds with the stability of the **FAB** derivative demonstrated in chapter 2.4. The ASA/SA ratio, determined by CE, slightly shifted on behalf of SA, possibly due to the basic buffer used as a background electrolyte. Even though the **FAB** derivative cannot migrate in an electric field, and thus, its detection was not possible during the drug release experiment using CE, measurement confirmed the slow release of ASA and SA from the polymer conjugate **P1-FAB** (up to 23% of SA is released at pH 7.4 within 72 h). Sufficient stability at physiological conditions can secure safe transport in the bloodstream, making the **P1-FAB** conjugate promising for *in vivo* application. After accumulation in inflammatory tissue, ASA and SA should be slowly released by hydrolysis or by the action of enzymes.

SAH release from polymer conjugate **P3-SAH** was assessed by organic phase extraction and CE. For the extraction method, it was necessary to determine the extraction coefficient of the SAH molecule into DCM because of poor SAH transition into the organic phase (ethyl acetate, DCM). Despite that, it was possible to determine SAH release from the polymer conjugate with almost all SAH released within 4 h at pH 5.0, and about 30% of SAH was released at pH 7.4 within 24 h (Fig. 2A). Moreover, SAH release was confirmed by CE (Fig. 2B). The **P3-SAH** conjugate is promising for the treatment of localized inflammation due to its favorable release profile.

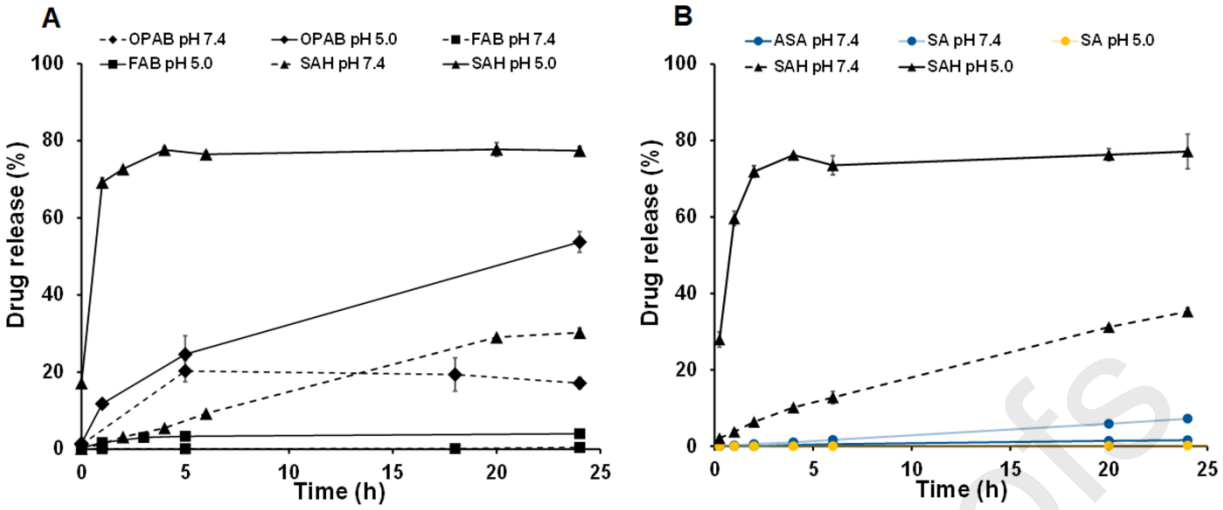

Figure 2. Drug release from polymer conjugates P1-FAB, P1-OPAB and P3-SAH incubated in 0.15 M phosphate buffers at 37°C. **A.** Organic phase extraction – P1-FAB (release of FAB), P1-OPAB (release of OPAB), P3-SAH (release of SAH); **B.** Capillary electrophoresis – P1-FAB (release of ASA, SA), P3-SAH (release of SAH).

2.6 *In vitro* biological properties of low-molecular-weight compounds and their polymer conjugates

To determine the cytotoxicity and biological effects of ASA and SAH polymer conjugates, and possible byproducts of their degradation, we performed two cytotoxicity assays and one assay monitoring NO production as an indicator of ongoing inflammatory response in macrophages. First, the safety and the anti-inflammatory effects of linkers HB, HBA, and HFB were evaluated since they may be released from ASA derivatives during the *in vitro* experiments and thus affect the results. The cytotoxicity was determined by the measurement of potential acute cytotoxicity by the LDH assay and the evaluation of overall cell viability by the MTT assay, showing that the linkers were not cytotoxic (Fig. 3A and B). Subsequently, the anti-inflammatory potential of the linkers was tested using the Griess assay. Interestingly, the results revealed the anti-inflammatory potential of all linkers in a dose-dependent manner as they decreased NO production by LPS-activated RAW 264.7 cells (Fig. 3C). The anti-inflammatory potential of linkers HBA and HFB was described previously[50,51]. They suppress NO production by specific inhibition of the expression of inducible iNOS and COX-2 in LPS-activated RAW 264.7 cells.

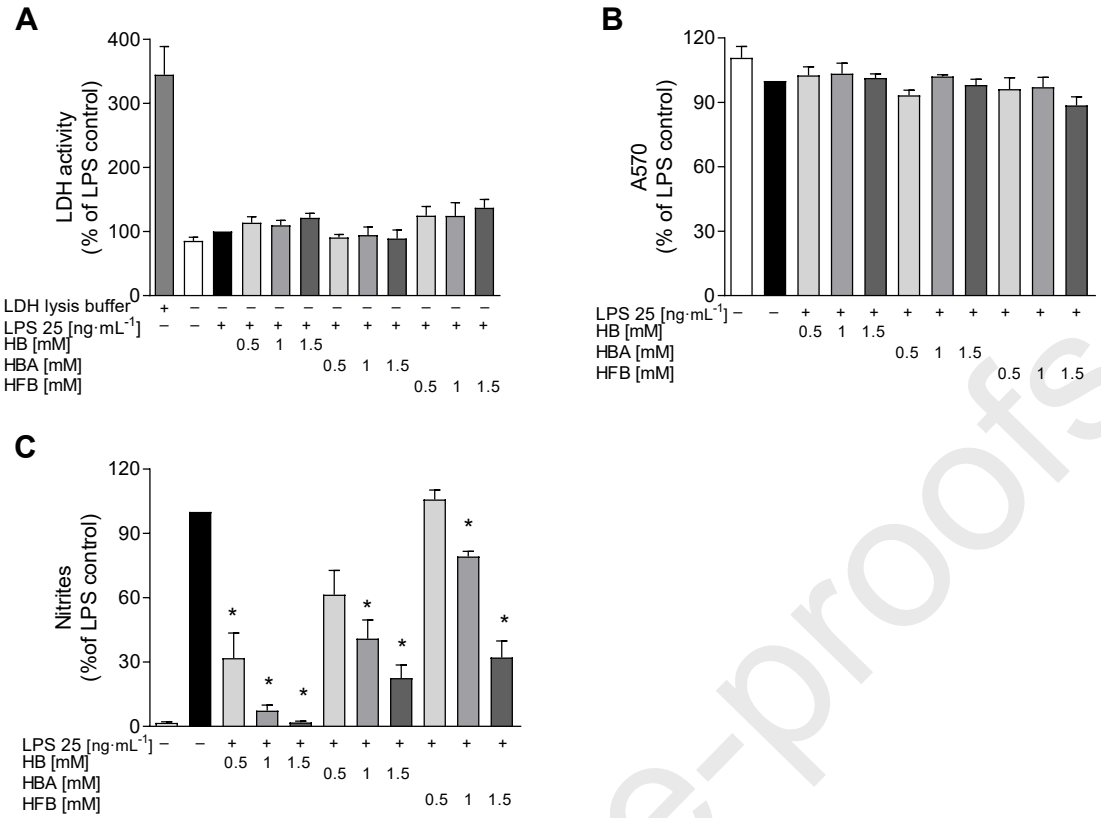

Figure 3: Effects of linkers on RAW 264.7 cell viability and NO production. The cells were pre-treated with the compounds for 60 min before the addition of LPS (25 ng·mL^{-1}). **A:** Determination of LDH; **B:** MTT assay; **C:** Griess assay. Data were converted to a percent of the LPS control and expressed as the mean ± SEM. One sample t-test was used to analyze the significance of obtained data comparing separately the effect of each compound with an activated control. The Bonferroni correction of the p-value for multiple comparisons was performed; * $p < 0.05$, n = 2-4.

The potential acute cytotoxicity of SAH, ASA, SA, and their polymer conjugates was evaluated by the measurement of LDH, protein content, and the MTT assay. **P1-OPAB** showed significant acute cytotoxicity (Fig. 4), which was confirmed by LDH and MTT assays. This result was further supported by the microscopic visualization of the detachment of RAW 264.7 cells from the flask surface (Fig. S3), resulting in cell death and, therefore, a lower protein content. The cytotoxicity was not caused by the released HFB linker as the linker is not toxic (Fig. 3A and B) but was most probably caused by the **OPAB** derivate, thus, **P1-OPAB** was excluded from further studies.

A slight but significant acute cytotoxicity of SAH was observed in the LDH assay (Fig. 4A); however, it was not confirmed by protein measurement or by the MTT assay (Figs. 4B and C). ASA, SA, **P3-SAH**, and polymer **P1** showed no cytotoxicity.

Although the main mechanism of action of ASA is COX inhibition by its acetyl residue[52], several studies showed that ASA also influences the activation of NF-κb signaling pathway[9,10]. Therefore, we evaluated the anti-inflammatory potential of the compounds by measurement of NO in the culture media. The analysis showed a dose-dependent inhibition of NO production by the tested compounds (Fig. 5). Some of the previous studies used a higher concentration of ASA of up to 20 mM with an IC_{50} of 3 mM for RAW 264.7 cells[53,54]. However, we observed the effective inhibition in a concentration as low as 0.5 mM for ASA, SA, SAH and **P3-SAH**. Polymer conjugate **P1-FAB** showed effective inhibition at 1.5 mM probably due to the slow ASA/SA release from **P1-FAB** in contrast to **P3-SAH**, where most SAH is released within 24 h (Fig. 2). Further, the hydrazone bond in **P1-FAB** is almost stable, especially at pH 7.4, thus, HBA would be released only negligibly *in vitro,* and the anti-inflammatory effect of **P1-FAB** could be ascribed to the released ASA/SA (chapter 2.5). The copolymer precursor **P1** did not show any significant effect on cell viability or NO production (Figs. 4 and 5).

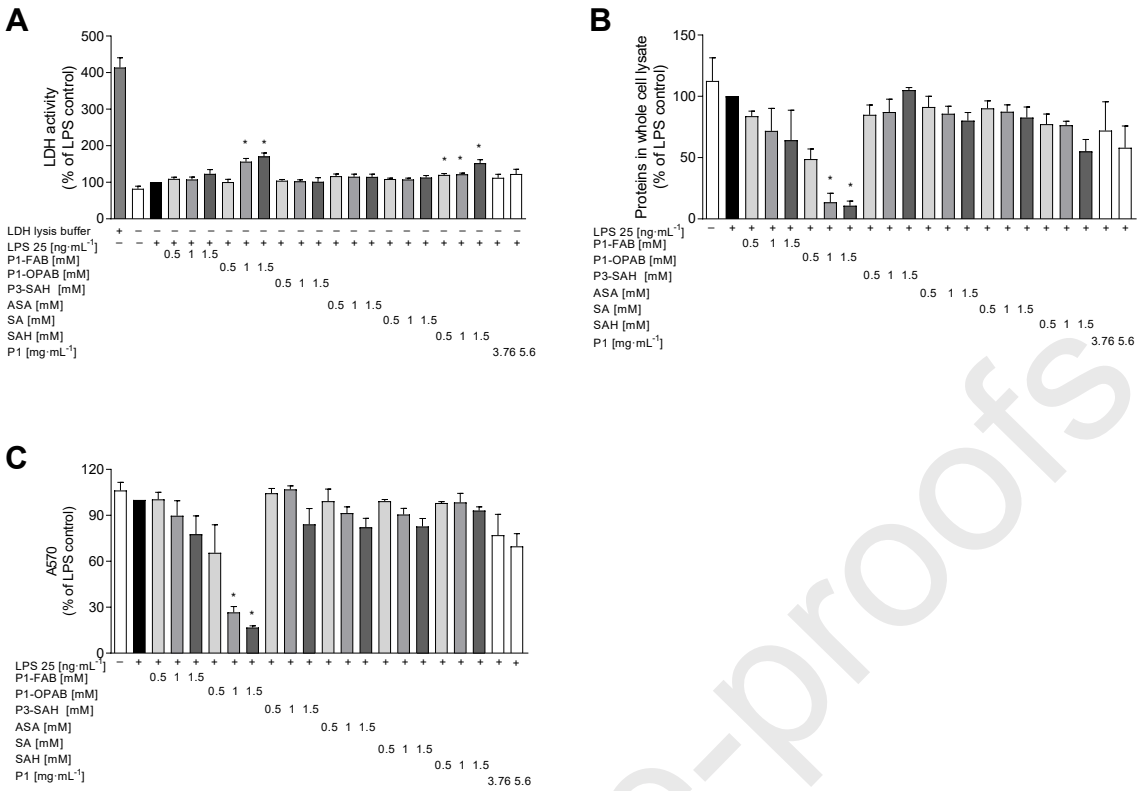

Figure 4: Effects of the polymer conjugates with ASA derivatives or SAH on the viability of RAW 264.7 cells. The cells were pre-treated with compounds for 60 min before the addition of LPS (25 ng·mL^{-1}). **A:** Determination of LDH; **B:** Determination of protein concentration; **C:** MTT assay. Data were converted to a percent of the LPS control and expressed as the mean ± SEM. One sample t-test was used to analyze the significance of obtained data comparing separately the effect of each compound with an activated control; the Bonferroni correction of the p-value for multiple comparisons was performed; * $p < 0.05$, $n = 4 – 5$. The concentration in mM by the polymer conjugates (P1-FAB, P1-OPAB, P3-SAH) corresponds to the concentration of the active molecule (i.e. ASA, or SAH).

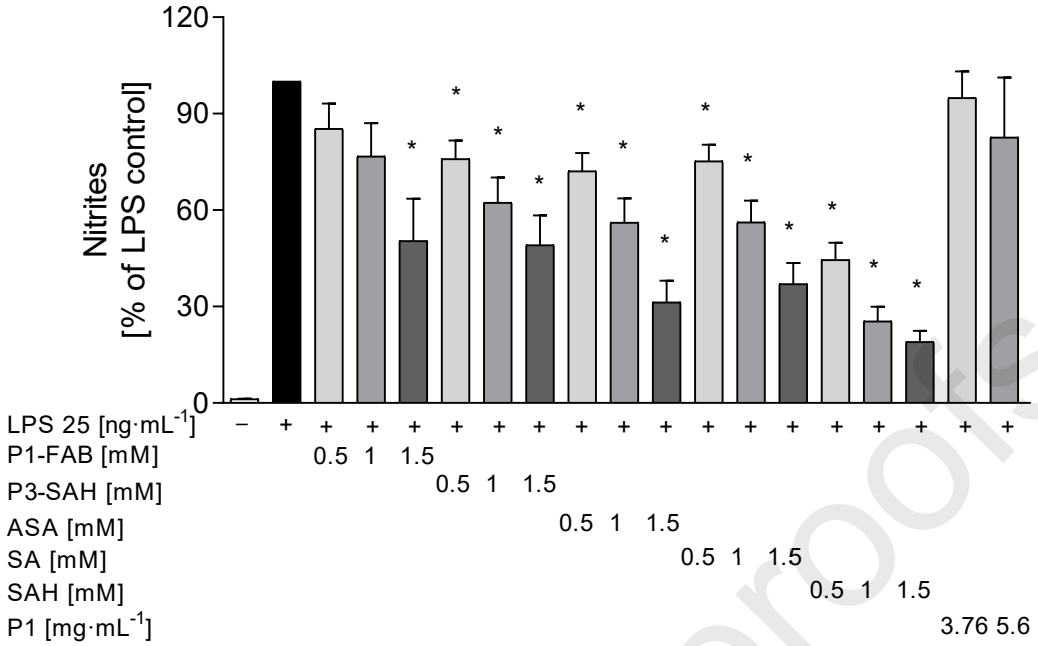

Figure 5: Effect of the polymer conjugates with ASA derivatives or SAH on the inflammatory response of activated RAW 264.7 cells. The cells were pre-treated with compounds for 60 min before the addition of LPS (25 ng·mL^{-1}). The content of nitrites in culture media was measured after 24 h incubation and data were converted to a percent of the LPS control and expressed as the mean ± SEM. One sample t-test was used to analyze the significance of obtained data comparing separately the effect of each compound with an activated control; the Bonferroni correction of the p-value for multiple comparisons was performed; * $p < 0.05$, $n = 4 – 5$. The concentration in mM by the polymer conjugates (P1-FAB, P3-SAH) corresponds to the concentration of the active molecule (i.e. ASA, or SAH).

The COX-1 and COX-2 inhibitory potential of polymer conjugates (**P1-FAB**, **P3-SAH)**, and all low-molecular-weight compounds potentially releasable from these conjugates (ASA, SA, SAH, HBA, **FAB**) were assessed showing that only ASA, SA, SAH, and polymer conjugate **P3-SAH** inhibited COX-1 (Fig. 6A). Low-molecular-weight SAH and **P3-SAH** preincubated for 24 h (to ensure the release of SAH from the conjugate) showed the most effective inhibition at 1.5 mM, with inhibition rates of 80% and 82%, respectively. Interestingly, low but significant ($p < 0.01$) levels of inhibition were detected for **P3**, probably due to the slight interaction of multiple presentation of COV acid-based polymer side chains with COX-1. Only ASA, SAH, and preincubated **P3-SAH** inhibited COX-2 (Fig. 6B). However, ASA was effective at a concentration of 1.0 mM or above. There was no significant difference in COX-1 or COX-2

inhibition between free SAH and SAH released from the conjugate during preincubation, confirming that SAH retains its biological activity after binding to the polymer and its subsequent release. Moreover, we identified SAH and SAH-releasing **P3-SAH** as the most potent inhibitors of COX-1 and COX-2. HBA, **FAB**, and polymer conjugate **P1-FAB** exerted no inhibitory effects on COX-1 or COX-2. Although HBA demonstrated anti-inflammatory activity (Fig. 3), its biological effect comprises in the inhibition of COX-2 expression.[50] **P1-FAB** failed to inhibit COX enzymes even after 72-hour preincubation, probably because of an insufficient amount of ASA/SA released from the conjugate. The release of ASA/SA from **P1-FAB** was slow (Fig. 2B) but could be altered by the different linkers, enabling faster release of the active molecule. **FAB** has already been published but there is no available biological data.[46]

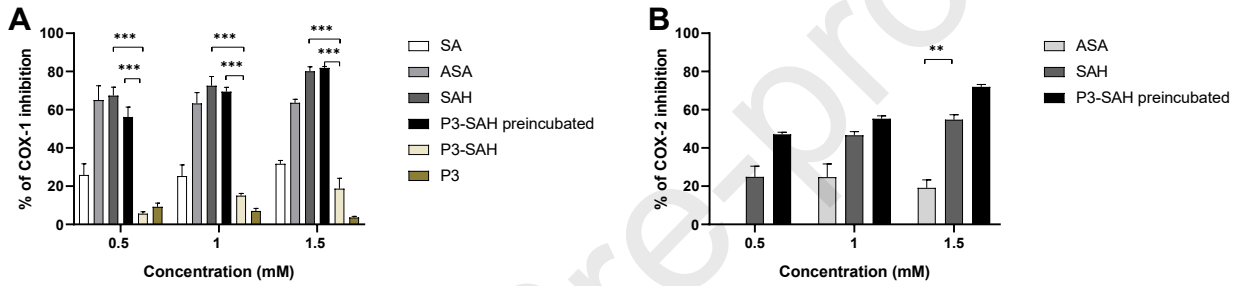

Figure 6. COX-1 and COX-2 inhibition. **A.** COX-1 inhibition. **B.** COX-2 inhibition. The concentrations of 0.5, 1.0, and 1.5 mM correspond to the concentration of the active molecule (ASA or SAH). The absorbance at 590 nm was measured kinetically and the COX-1 and COX-2 inhibition rates were calculated from an exponential phase. The results are normalized to the control and depicted as mean ± SEM. Multiple sample t-test was used to analyze the significance of obtained data; ***$p < 0.001$, $n = 3$.

As mentioned before, ASA was reported to inhibit the secretion of pro-inflammatory mediators, e.g. TNF-α, via suppression of lipopolysaccharide-inducible NF-κB binding to an NF-κB binding site in the TNF-α gene promoter.[55] Therefore, we tested the ability of ASA released from **P1-FAB** conjugate to inhibit TNF-α secretion. The effect of different concentrations of the **P1-FAB** on TNF-α secretion of stimulated RAW 264.7 cells by LPS or LPS+IFNγ is depicted in Fig. 7. In both treatments, the **P1-FAB** induced a marked and significant decrease in TNF-α secretion ($P \leq 0.0001$) compared to the control. At the maximum concentration of the **P1-FAB**, the inhibition of TNF-α secretion was close to 50% compared to the control. The polymer precursor **P1** did not affect TNF-α secretion (data not shown).

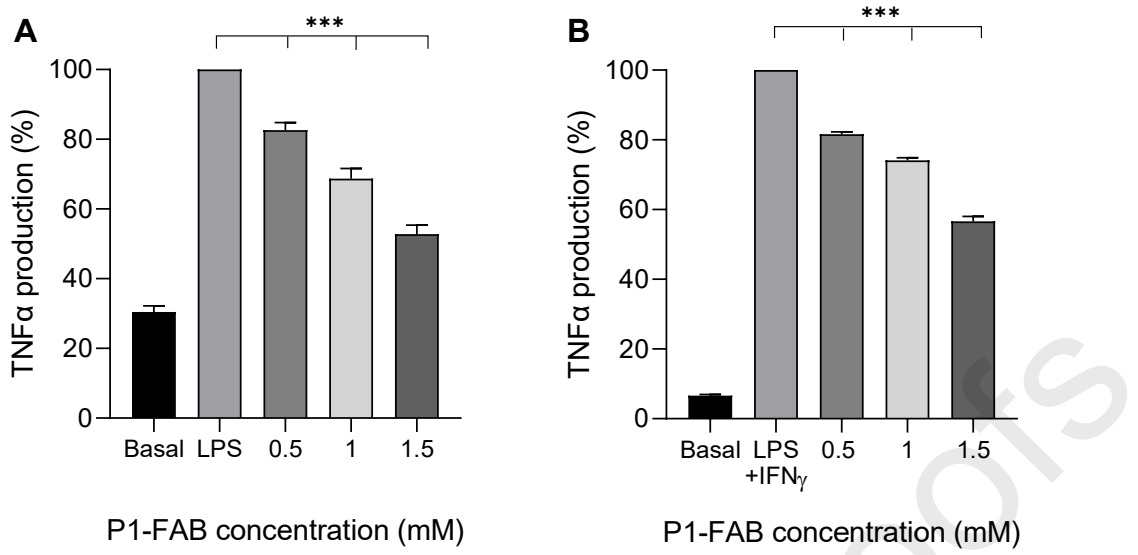

Figure 7. Inhibition of TNF-α production in RAW 264.7 cells using polymer conjugate P1-FAB. Cells were activated by **A.** LPS or **B.** LPS + IFNγ. Inhibition of TNF-α production was measured after 24 h incubation. The concentrations 0.5, 1.0, and 1.5 mM correspond to the concentration of the active molecule (ASA). The results are depicted as mean ± SEM. One-way ANOVA was used to analyze the significance of obtained data; ***$p < 0.001$, $n = 15$.

Conclusion

Biocompatible water-soluble polymer conjugates based on HPMA copolymers, enabling the controlled release of ASA-based anti-inflammatory drugs under specific stimuli were successfully designed, synthesized, and evaluated. We focused on their chemical characterization, behavior at physiological conditions, and *in vitro* biological properties. The most potent anti-inflammatory compounds were those carrying SAH bound via a pH-sensitive hydrazone bond to the polymer carrier allowing selective SAH release in the acidic inflammatory environment. These polymer conjugates were nontoxic, successfully inhibited COX-1 and COX-2, and reduced the level of the pro-inflammatory mediator NO. The polymer bearing an ester-bound ASA was found to be a useful ASA-drug delivery system with long-term release of the ASA/SA mixture and effectively inhibited the production of pro-inflammatory mediators TNF-α and NO. Due to their water solubility, suitable hydrodynamic size, and molecular weight, these conjugates could be preferentially accumulated in inflamed tissue through ELVIS effect, thereby reducing potential side effects and dosing. Moreover, after fulfilling their role, the polymer carriers should be effectively eliminated by renal filtration from the body. Based on the anti-inflammatory activity of SAH- and ASA-containing

nanotherapeutics and the benefits of HPMA-based nanotherapeutics, we will consider further testing of *in vivo* activity for the treatment of inflammatory diseases since the effective and safe treatment of inflammation is still a great task of modern medicine and our nanotherapeutics could be beneficial for future use. Moreover, the developed polymer conjugates enable the transport of a combination of therapeutics, which could be significant both in the treatment of inflammation and cancer, where inflammation also plays an important role in carcinogenesis.

Acknowledgment

This work was supported by the Ministry of the Health of the Czech Republic (NU20-08-00255). D. Rubanová is a Brno Ph.D. Talent Scholarship Holder – Funded by the Brno City Municipality. The authors also thank Olga Kočková for the MALDI-TOF measurement.

Conflict of interest

The authors declare no conflict of interest.

Supplementary Information (SI) available: Figure S1-S3; ^{1}H NMR characterization of polymer conjugates (S1), Numbering of aromatic atoms (ASA derivatives) in NMR assignments (S2), Representative images of RAW 264.7 morphology after selected treatments (S3).

For Table of Contents Only

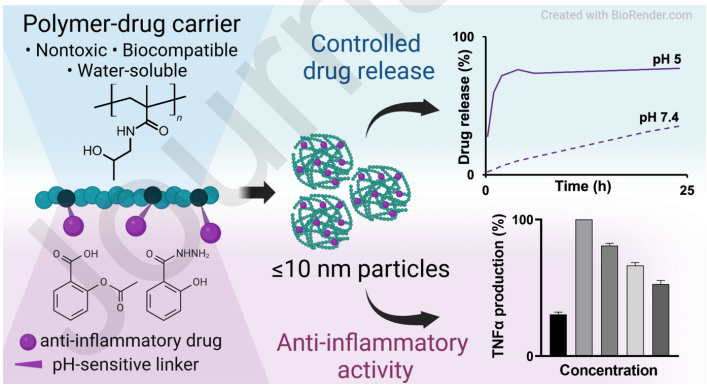

References

(1) Montinari, M. R.; Minelli, S.; De Caterina, R. The First 3500 years of Aspirin History from Its Roots – A Concise Summary. *Vascul. Pharmacol.* **2019**, *113* (October 2018), 1–8. https://doi.org/10.1016/j.vph.2018.10.008.

(2) Roberge, S.; Bujold, E.; Nicolaides, K. H. Aspirin for the Prevention of Preterm and Term Preeclampsia: Systematic Review and Metaanalysis. *Am. J. Obstet. Gynecol.* **2018**, *218* (3), 287–293. https://doi.org/10.1016/j.ajog.2017.11.561.

(3) Rothwell, P.; Cook, N.; Gaziano, J.; Price, J.; Belch, J.; Roncaglioni, M.; Morimoto, T.; Mehta, Z. Effects of Aspirin on Risks of Vascular Events and Cancer According to Bodyweight and Dose: Analysis of Individual Patient Data from Randomised Trials. *Lancet* **2018**, *392* (10145), 387–399. https://doi.org/10.1016/S0140-6736(18)31133-4.

(4) The ASCEND Study Collaborative Group. Effects of Aspirin for Primary Prevention in Persons with Diabetes Mellitus. *N. Engl. J. Med.* **2018**, *379* (16), 1529–1539. https://doi.org/10.1056/nejmoa1804988.

(5) Lu, J.; Cong, T.; Wen, X.; Li, X.; Du, D.; He, G.; Jiang, X. Salicylic Acid Treats Acne Vulgaris by Suppressing AMPK/SREBP1 Pathway in Sebocytes. *Exp. Dermatol.* **2019**, *28* (7), 786–794. https://doi.org/10.1111/exd.13934.

(6) Zidar, N.; Odar, K.; Glavac, D.; Jerse, M.; Zupanc, T.; Stajer, D. Cyclooxygenase in Normal Human Tissues - Is COX-1 Really a Constitutive Isoform, and COX-2 an Inducible Isoform? *J. Cell. Mol. Med.* **2009**, *13* (9B), 3753–3763. https://doi.org/10.1111/j.1582-4934.2008.00430.x.

(7) Yasojima, K.; Schwab, C.; McGeer, E. G.; McGeer, P. L. Distribution of Cyclooxygenase-1 and Cyclooxygenase-2 mRNAs and Proteins in Human Brain and Peripheral Organs. *Brain Res.* **1999**, *830* (2), 226–236. https://doi.org/10.1016/s0006-8993(99)01389-x.

(8) O'Neill, G. P.; Ford-Hutchinson, A. W. Expression of mRNA for Cyclooxygenase-1 and Cyclooxygenase-2 in Human Tissues. *FEBS Lett.* **1993**, *330* (2), 157–160. https://doi.org/10.1016/0014-5793(93)80263-T.

(9) Yin, M. J.; Yamamoto, Y.; Gaynor, R. B. The Anti-Inflammatory Agents Aspirin and Salicylate Inhibit the Activity of I(Kappa)B Kinase-Beta. *Nature* **1998**, *396* (6706), 77–80. https://doi.org/10.1038/23948.

(10) Liu, Y.; Fang, S.; Li, X.; Feng, J.; Du, J.; Guo, L.; Su, Y.; Zhou, J.; Ding, G.; Bai, Y.; Wang, S.; Wang, H.; Liu, Y. Aspirin Inhibits LPS-Induced Macrophage Activation via the NF-kappaB Pathway. *Sci. Rep.* **2017**, *7* (1), 1–11. https://doi.org/10.1038/s41598-017-10720-4.

(11) Serhan, C. N. Lipoxins and Aspirin-Triggered 15-Epi-Lipoxins Are the First Lipid Mediators of Endogenous Anti-Inflammation and Resolution. *Prostaglandins Leukot. Essent. Fat. Acids* **2005**, *73* (3–4), 141–162. https://doi.org/10.1016/j.plefa.2005.05.002.

(12) Gilligan, M. M.; Gartung, A.; Sulciner, M. L.; Norris, P. C.; Sukhatme, V. P.; Bielenberg, D. R.; Huang, S.; Kieran, M. W.; Serhan, C. N.; Panigrahy, D. Aspirin-Triggered Proresolving Mediators Stimulate Resolution in Cancer. *Proc. Natl. Acad. Sci. U. S. A.* **2019**, *116* (13), 6292–6297. https://doi.org/10.1073/pnas.1804000116.

(13) Kopeček, J.; Yang, J. Polymer Nanomedicines. *Adv. Drug Deliv. Rev.* **2020**, *156*, 40–64.

https://doi.org/10.1016/j.addr.2020.07.020.

(14) Matsumura, Y.; Maeda, H. A New Concept for Macromolecular Therapeutics in Cancer Chemotherapy: Mechanism of Tumoritropic Accumulation of Proteins and the Antitumor Agent Smancs. *Cancer Res.* **1986**, *46* (8), 6387–6392. PMID: 2946403.

(15) Brusini, R.; Varna, M.; Couvreur, P. Advanced Nanomedicines for the Treatment of Inflammatory Diseases. *Adv. Drug Deliv. Rev.* **2020**, *157*, 161–178. https://doi.org/10.1016/j.addr.2020.07.010.

(16) Li, P.; Wang, C.; Huo, H.; Xu, C.; Sun, H.; Wang, X.; Wang, L.; Li, L. Prodrug-Based Nanomedicines for Rheumatoid Arthritis. *Discov. Nano* **2024**, *19* (1). https://doi.org/10.1186/s11671-023-03950-1.

(17) Wang, D.; Miller, S. C.; Liu, X. M.; Anderson, B.; Wang, X. S.; Goldring, S. R. Novel Dexamethasone-HPMA Copolymer Conjugate and Its Potential Application in Treatment of Rheumatoid Arthritis. *Arthritis Res. Ther.* **2007**, *9* (1), 1–9. https://doi.org/10.1186/ar2106.

(18) Espinosa-Cano, E.; Aguilar, M. R.; Portilla, Y.; Barber, D. F.; Román, J. S. Anti-Inflammatory Polymeric Nanoparticles Based on Ketoprofen and Dexamethasone. *Pharmaceutics* **2020**, *12* (8), 1–18. https://doi.org/10.3390/pharmaceutics12080723.

(19) Paul, W.; Sharma, C. P. Acetylsalicylic Acid Loaded Poly(vinyl alcohol) Hemodialysis Membranes: Effect of Drug Release on Blood Compatibility and Permeability. *J. Biomater. Sci. Polym. Ed.* **1997**, *8* (10), 755–764. https://doi.org/10.1163/156856297X00290.

(20) You, X.; Wang, L.; Wang, L.; Wu, J. Rebirth of Aspirin Synthesis By-Product: Prickly Poly(Salicylic Acid) Nanoparticles as Self-Anticancer Drug Carrier. *Adv. Funct. Mater.* **2021**, *31* (33), 1–13. https://doi.org/https://doi.org/10.1002/adfm.202100805.

(21) Akkad, S.; Serpell, C. J. Degradable Polymers and Nanoparticles Built from Salicylic Acid. *Macromol. Rapid Commun.* **2018**, *39* (14), 1–5. https://doi.org/10.1002/marc.201800182.

(22) Chandorkar, Y.; Bhaskar, N.; Madras, G.; Basu, B. Long-Term Sustained Release of Salicylic Acid from Cross-Linked Biodegradable Polyester Induces a Reduced Foreign Body Response in Mice. *Biomacromolecules* **2015**, *16* (2), 636–649. https://doi.org/10.1021/bm5017282.

(23) Castillo-Miranda, C. A.; Castro-Guerrero, C. F.; Velasco-Ocejo, H. A.; Gonzalez-Sanchez, J. A.; Flores-Cerda, G. O.; Ramos-Galvan, C. E.; Rivera-Armenta, J. L.; Morales-Cepeda, A. B. Acetylsalicylic Acid (ASA) on Hydroxyethylcellulose/Polyacrylamide Gel (HEC/PAAm) as a Proposal for a Dermatological Compress: Mathematical Modeling of ASA Release Kinetics. *Int. J. Polym. Sci.* **2019**, *2019* (1), 1–10. https://doi.org/https://doi.org/10.1155/2019/4597641.

(24) Dasgupta, Q.; Chatterjee, K.; Madras, G. Controlled Release of Salicylic Acid from Biodegradable Cross-Linked Polyesters. *Mol. Pharm.* **2015**, *12* (9), 3479–3489. https://doi.org/10.1021/acs.molpharmaceut.5b00515.

(25) Erdmann, L.; Uhrich, K. E. Synthesis and Degradation Characteristics of Salicylic Acid-Derived Poly(anhydride-esters). *Biomaterials* **2000**, *21* (19), 1941–1946. https://doi.org/10.1016/S0142-9612(00)00073-9.

(26) Cai, Q.; Zhu, K. J.; Zhang, J. Salicylic Acid and PEG-Contained Polyanhydrides: Synthesis, Characterization, and In Vitro Salicylic Acid Release. *Drug Deliv. J. Deliv. Target. Ther. Agents* **2005**, *12* (2), 97–102. https://doi.org/10.1080/10717540490446107.

(27) Jantas, R.; Draczyński, Z.; Herczyńska, L.; Stawski, D. Poly(vinyl alcohol)-Salicylic Acid Conjugate: Synthesis and Characterization. *Am. J. Polym. Sci.* **2012**, *2* (5), 79–84. https://doi.org/10.5923/j.ajps.20120205.01.

(28) Liu, Y.; Du, J.; Peng, P.; Cheng, R.; Lin, J.; Xu, C.; Yang, H.; Cui, W.; Mao, H.; Li, Y.; Geng, D. Regulation of the Inflammatory Cycle by a Controllable Release Hydrogel for Eliminating Postoperative Inflammation after Discectomy. *Bioact. Mater.* **2021**, *6* (1), 146–157. https://doi.org/10.1016/j.bioactmat.2020.07.008.

(29) Wang, F.; Huang, P.; Huang, D.; Hu, Y.; Ma, K.; Cai, X.; Jiang, T. Preparation and Functionalization of Acetylsalicylic Acid Loaded Chitosan/Gelatin Membranes from Ethanol-based Suspensions via Electrophoretic Deposition. *J. Mater. Chem. B* **2018**, *6* (15), 2304–2314. https://doi.org/10.1039/c7tb03033a.

(30) Ebru Kılıçay, Birten Çakmaklı, Baki Hazer, Emir Baki Denkbaş, B. A. Acetylsalicylic Acid Loading and Release Studies of the PMMA-g-Polymeric Oils/Oily Acids Micro and Nanospheres. *J. Appl. Polym. Sci.* **2011**, *119* (3), 1610–1618. https://doi.org/10.1002/app.32825.

(31) Li, F.-M.; Li, G.-W.; Wang, S.; Feng, X.-D.; Gu, Z.-W. Synthesis of Biocompatible Polymers with Aspirin-Moieties for Aspirin Delivery. *J. Bioact. Compat. Polym.* **1991**, *6* (2), 142–163. https://doi.org/10.1177/088391159100600203.

(32) Bakar, S. K.; Niazi, S. Stability of Aspirin in Different Media. *J. Pharm. Sci.* **1983**, *72* (9), 1024–1026. https://doi.org/10.1002/jps.2600720914.

(33) Klessig, D. F.; Tian, M.; Choi, H. W. Multiple Targets of Salicylic Acid and Its Derivatives in Plants and Animals. *Front. Immunol.* **2016**, *7* (MAY), 1–10. https://doi.org/10.3389/fimmu.2016.00206.

(34) Quan, L.; Zhang, Y.; Crielaard, B. J.; Dusad, A.; Lele, S. M.; Cristianne J. F., R.; Metselaar, J. M.; Kostkova, H.; Etrych, T.; Ulbrich, K.; Kiessling, F.; Mikuls, T. R.; Hennink, W. E.; Storm, G.; Lammers, T.; Wang, D. Nanomedicines for Inflammatory Arthritis : Head-to-Head Comparison of Glucocorticoid-Containing Polymers, Micelles, and Liposomes. *ACS Nano* **2013**, *8* (1), 458–466. https://doi.org/https://doi.org/10.1021/nn4048205.

(35) Ebbesen, M. F.; Bienk, K.; Deleuran, B. W.; Howard, K. A. Extended Blood Circulation and Joint Accumulation of a p(HPMA-co-AzMA)-based Nanoconjugate in a Murine Model of Rheumatoid Arthritis. *Mol. Cell. Ther.* **2014**, *2* (1), 29. https://doi.org/10.1186/2052-8426-2-29.

(36) Libánská, A.; Randárová, E.; Lager, F.; Renault, G.; Scherman, D.; Etrych, T. Polymer Nanomedicines with pH-Sensitive Release of Dexamethasone for the Localized Treatment of Inflammation. *Pharmaceutics* **2020**, *12* (8), 1–19. https://doi.org/10.3390/pharmaceutics12080700.

(37) Tondelier, D.; Brouillard, F.; Lipecka, J.; Labarthe, R.; Bali, M.; Costa De Beauregard, M. A.; Torossi, T.; Cougnon, M.; Edelman, A.; Baudouin-Legros, M. Aspirin and Some Other Nonsteroidal Anti-Inflammatory Drugs Inhibit Cystic Fibrosis Transmembrane

Conductance Regulator Protein Gene Expression in T-84 Cells. *Mediators Inflamm.* **1999**, *8* (4–5), 219–227. https://doi.org/10.1080/09629359990388.

(38) Chytil, P.; Etrych, T.; Kříž, J.; Šubr, V.; Ulbrich, K. *N*-(2-Hydroxypropyl)methacrylamide-based Polymer Conjugates with pH-controlled Activation of Doxorubicin for Cell-Specific or Passive Tumour Targeting. Synthesis by RAFT Polymerisation and Physicochemical Characterisation. *Eur. J. Pharm. Sci.* **2010**, *41* (3–4), 473–482. https://doi.org/10.1016/j.ejps.2010.08.003.

(39) Ulbrich, K.; Etrych, T.; Chytil, P.; Jelínková, M.; Říhová, B. Antibody-Targeted Polymer-Doxorubicin Conjugates with pH-Controlled Activation. *J. Drug Target.* **2004**, *12* (8), 477–489. https://doi.org/10.1080/10611860400011869.

(40) Ishitake, K.; Satoh, K.; Kamigaito, M.; Okamoto, Y. Stereogradient Polymers Formed by Controlled/Living Radical Polymerization of Bulky Methacrylate Monomers. *Angew. Chemie - Int. Ed.* **2009**, *48* (11), 1991–1994. https://doi.org/10.1002/anie.200805168.

(41) Perrier, S.; Takolpuckdee, P.; Mars, C. A. Reversible Addition - Fragmentation Chain Transfer Polymerization: End Group Modification for Functionalized Polymers and Chain Transfer Agent Recovery. *Macromolecules* **2005**, *38*, 2033–2036. https://doi.org/10.1021/ma047611m.

(42) Bláhová, M.; Randárová, E.; Konefał, R.; Nottelet, B.; Etrych, T. Graft Copolymers with Tunable Amphiphilicity Tailored for Efficient Dual Drug Delivery via Encapsulation and pH-Sensitive Drug Conjugation. *Polym. Chem.* **2020**, *11* (27), 4438–4453. https://doi.org/10.1039/d0py00609b.

(43) Koziolová, E.; Kostka, L.; Kotrchová, L.; Šubr, V.; Konefal, R.; Nottelet, B.; Etrych, T. *N*-(2-Hydroxypropyl)methacrylamide-based Linear, Diblock, and Starlike Polymer Drug Carriers: Advanced Process for Their Simple Production. *Biomacromolecules* **2018**, *19* (10), 4003–4013. https://doi.org/10.1021/acs.biomac.8b00973.

(44) Rubanová, D.; Skoroplyas, S.; Libánská, A.; Randárová, E.; Bryja, J.; Chorvátová, M.; Etrych, T.; Kubala, L. Therapeutic Activity and Biodistribution of a Nano-Sized Polymer-Dexamethasone Conjugate Intended for the Targeted Treatment of Rheumatoid Arthritis. *Nanomedicine Nanotechnology, Biol. Med.* **2024**, *55*, pages not assigned. https://doi.org/https://doi.org/10.1016/j.nano.2023.102716.

(45) Lidický, O.; Šírová, M.; Etrych, T. HPMA Copolymer-based Polymer Conjugates for the Delivery and Controlled Release of Retinoids. *Physiol. Res.* **2016**, *65*, S233–S241. https://doi.org/10.33549/physiolres.933425.

(46) Chang-Xiao, S. U.; Mouscadet, J. F.; Chiang, C. C.; Tsai, H. J.; Hsu, L. Y. HIV-1 Integrase Inhibition of Biscoumarin Analogues. *Chem. Pharm. Bull.* **2006**, *54* (5), 682–686. https://doi.org/10.1248/cpb.54.682.

(47) Park, S.; Lee, J.; Shin, K. J.; Seo, J. H. Aspirination of α-Aminoalcohol (Sarpogrelate M1). *Molecules* **2016**, *21* (9), 1–9. https://doi.org/10.3390/molecules21091126.

(48) Chytil, P.; Hoffmann, S.; Schindler, L.; Kostka, L.; Ulbrich, K.; Caysa, H.; Mueller, T.; Mäder, K. Dual Fluorescent HPMA Copolymers for Passive Tumor Targeting with pH-Sensitive Drug Release II : Impact of Release Rate on Biodistribution. *J. Control. Release* **2013**, *172*, 504–512. https://doi.org/10.1016/j.jconrel.2013.05.008.

(49) Libánská, A.; Špringer, T.; Peštová, L.; Kotalík, K.; Konefał, R.; Šimonová, A.; Křížek,

T.; Homola, J.; Randárová, E.; Etrych, T. Using Surface Plasmon Resonance, Capillary Electrophoresis and Diffusion-Ordered NMR Spectroscopy to Study Drug Release Kinetics. *Commun. Chem.* **2023**, *6* (1), 1–12. https://doi.org/10.1038/s42004-023-00992-5.

(50) Lim, E. J.; Kang, H. J.; Jung, H. J.; Kim, K.; Lim, C. J.; Park, E. H. Anti-Inflammatory, Anti-Angiogenic and Anti-Nociceptive Activities of 4-Hydroxybenzaldehyde. *Biomol. Ther.* **2008**, *16* (3), 231–236. https://doi.org/10.4062/biomolther.2008.16.3.231.

(51) Jeong, J. B.; Jeong, H. J. Rheosmin, a Naturally Occurring Phenolic Compound Inhibits LPS-Induced iNOS and COX-2 Expression in RAW264.7 Cells by Blocking NF-kappaB Activation Pathway. *Food Chem. Toxicol.* **2010**, *48* (8–9), 2148–2153. https://doi.org/10.1016/j.fct.2010.05.020.

(52) Vane, J. R.; Botting, R. M. The Mechanism of Action of Aspirin. *Thromb. Res.* **2003**, *110* (5–6), 255–258. https://doi.org/10.1016/S0049-3848(03)00379-7.

(53) Amin, A. R.; Vyas, P.; Attur, M.; Leszczynska-Piziak, J.; Patel, I. R.; Weissmann, G.; Abramson, S. B. The Mode of Action of Aspirin-like Drugs: Effect on Inducible Nitric Oxide Synthase. *Proc. Natl. Acad. Sci. U. S. A.* **1995**, *92* (17), 7926–7930. https://doi.org/10.1073/pnas.92.17.7926.

(54) Kepka-Lenhart, D.; Chen, L. C.; Morris, S. M. Novel Actions of Aspirin and Sodium Salicylate: Discordant Effects on Nitric Oxide Synthesis and Induction of Nitric Oxide Synthase mRNA in a Murine Macrophage Cell Line. *J. Leukoc. Biol.* **1996**, *59* (6), 840–846. https://doi.org/10.1002/jlb.59.6.840.

(55) Shackelford, R. E.; Alford, P. B.; Xue, Y.; Thai, S. F.; Adams, D. O.; Pizzo, S. Aspirin Inhibits Tumor Necrosis Factor alpha Gene Expression in Murine Tissue Macrophages. *Mol. Pharmacol.* **1997**, *52* (3), 421–429. https://doi.org/10.1124/mol.52.3.421.

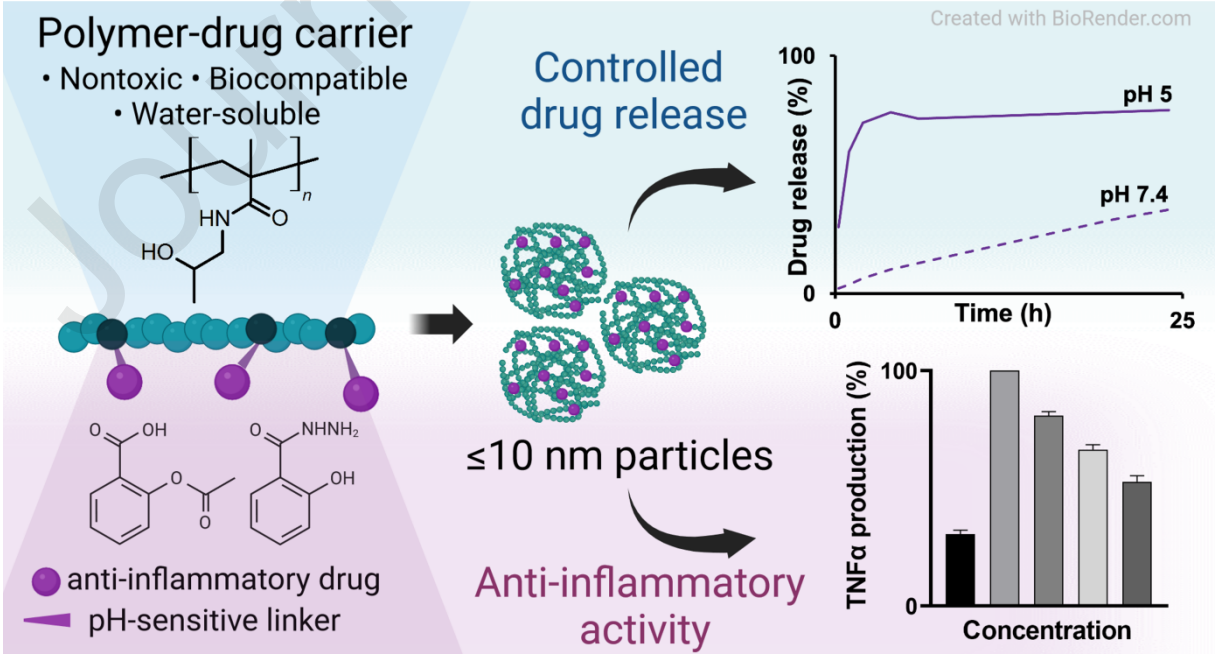

Declaration of competing interest

The authors declare that they have no known competing financial interests or personal relationships that could have appeared to influence the work reported in this paper.